BARC
NEWSLETTER

Slave arms of Advanced Servo Manipulator in Hot cell   29

CONTENTS
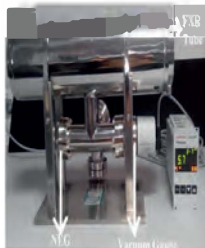
Indigenous Development of Sealed off Flash X-Ray Tube for 450 kV

Basanta Kumar Das, Rashmita Das, Partha Banerjee, Sukanta Mishra, Samir Sahoo, B. Gowri Sankar, Vijaya Laxmi Sethi, Ramanand Raman, Nitin Waghmare, M. Sankari, M. V. Suryanarayana, Archana Sharma
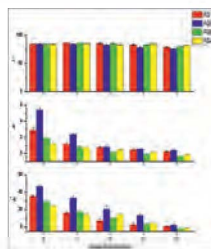
Pulse Power & Electromagnetics Division, Bhabha Atomic Research Centre, Atchutapuram, Visakhapatnam- 531011

Abstract

Sealed vacuum tubes have many advantages like easy transportation, low operation cost, less start up time etc. One sealed tube flash X-ray tube consisting of a diode configuration of tungsten anode and stainless steel cathode has been developed in our laboratory for operation up to 450 kV. All components of this tube, including high voltage insulator are compatible in ultra high vacuum. The tube is tested for X-ray generation for a dose of 10 mrad at a distance of 1 m from the X-ray window. The tube is tested for frequent operation with an interval of 2 minutes without vacuum degradation.

Introduction

Flash X-ray Radiography (FXR) is one of the few methods employed for high speed radiography of fast moving objects [1]. It is useful for non destructive testing of materials. For high quality electron beam, this device is operated at vacuum – below 10^{-6} mbar. Sealed off vacuum systems have many advantages like easy transportation, low operation cost, less start up time etc. A sealed off FXR tube is developed in our laboratory that is operated in high vacuum range of 10^{-7} mbar as that of a dynamically pumped system. This tube is of cold cathode type. This consists of a tapered anode of 1mm diameter made of tungsten and a ring shaped cathode of 10 mm whose inner diameter is made of SS. The anode and cathode assembly is housed in an SS 304 L tube. The tube structure itself acts as return current path. In cathode side of the tube, a vacuum interface of Aluminum disc is used as X-ray window. For high voltage insulation between the tube wall and the anode, one feed through made of natural

PEEK (Polyether ether ketone) is used. PEEK is selected on the basis of its low outgassing rate, dielectric strength, good mechanical strength and easy machinability. As the

dimensions of the vacuum tube are non standard and the requirement for PEEK to metal seal, vacuum sealing of Indium wire seal (IWS) is preferred over other methods. One 50 lit/s non
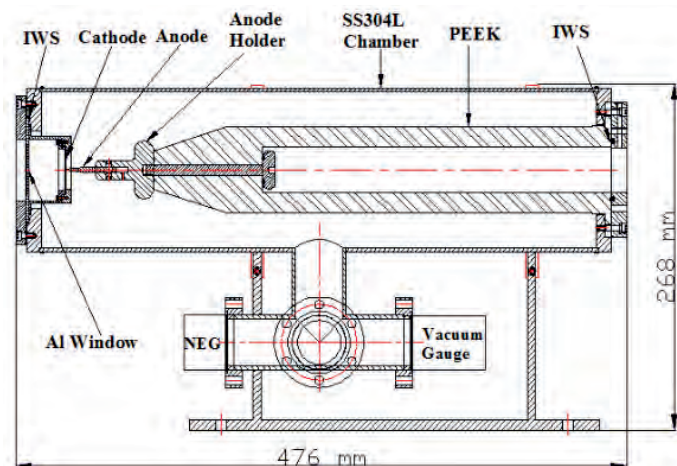

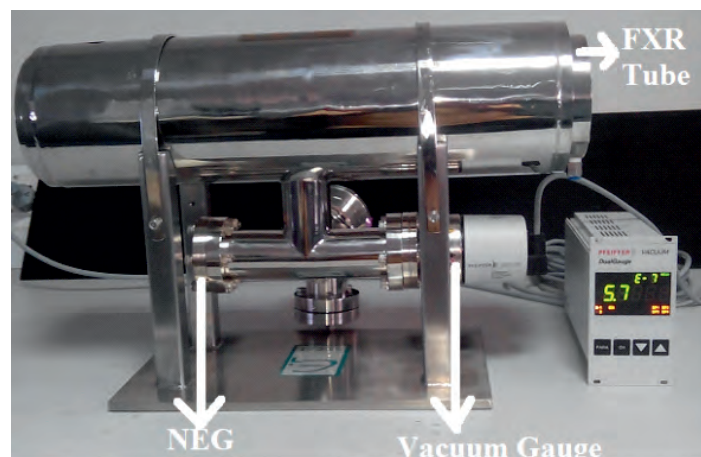Fig.1: Schematic diagram of the FXR tube

Fig. 2: Sealed off FXR tube

evaporable getter (NEG) is used for in situ pumping of the FXR tube in sealed off condition.

Methods

a. Sealing Procedure

The schematic diagram of the electrode arrangement is shown in the **Fig.1**. The photograph of the seal off FXR tube is shown in **Fig.2**. The whole assembly was leak tested with helium leak detection system. The leak rate was better than 1.1×10^{-10} mbar lit/sec. The assembly was mounted on a Turbo molecular pumping (TMP) station for creation of vacuum. After getting a base pressure of 1×10^{-6} mbar, baking of the vacuum system was started. For baking, silicon rubber insulated heating tapes were wrapped all over the vacuum chamber, including FXR tube. Baking was carried out for 24 hrs in discrete mode (~ 8 hrs per day) at a temperature of 110^{0} C. NEG was activated at the end of the baking cycle. During the pump down period, evolution of partial pressures of residual gases was measured by residual gas analyzer. After getting a base pressure in the order of 10^{-8} mbar, the FXR tube was isolated from the TMP station by 35 CF angle valve. The spectrum shown in **Fig.3** represents the partial pressures of the residual gases present in the system before baking. Before baking, the major contribution to the total pressure was from the water vapour. The presence of hydrogen is due to the dissociation of the water vapour at the ion source of the residual gas analyzer. The spectrum shown in **Fig.4** represents the partial pressures of the residual gases during baking. The highest value of hydrogen is due to the release from NEG during conditioning and activation and water vapor from the

vacuum chamber wall. Hydrogen release from NEG during heating and water vapor from vacuum chamber wall are natural phenomena. The water vapour sticks to the chamber wall due to weak Van der Waal's forces

which can be effectively removed by baking. **Fig.5** represents the partial pressure value of residual gases after baking and before FXR tube was isolated from the TMP.
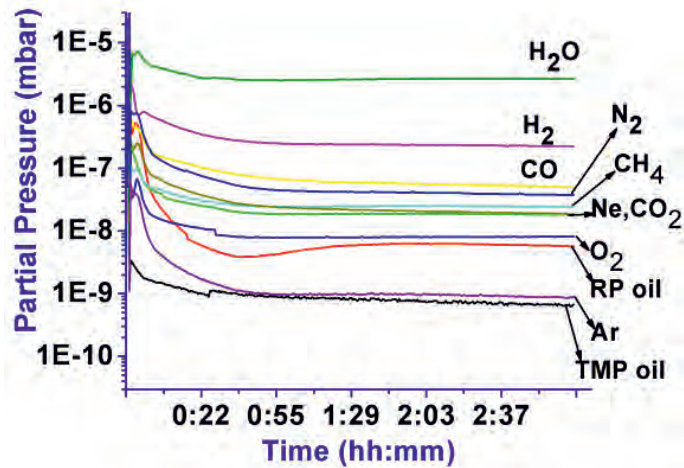

Fig. 3: Partial pressure of residual gases before baking.
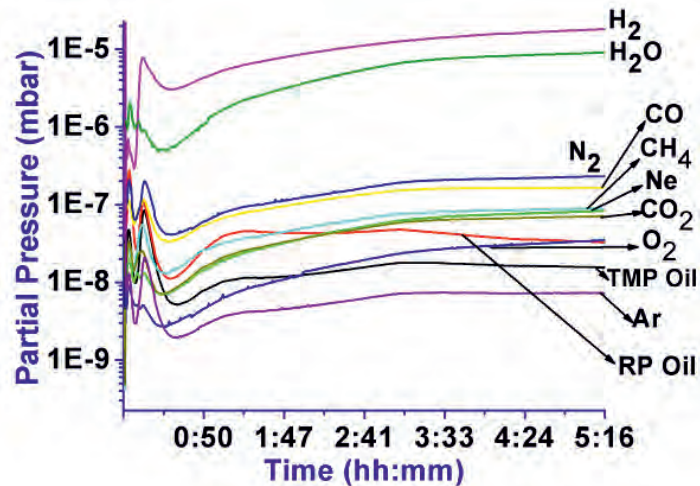

Fig. 4: Partial pressure of residual gases during baking.
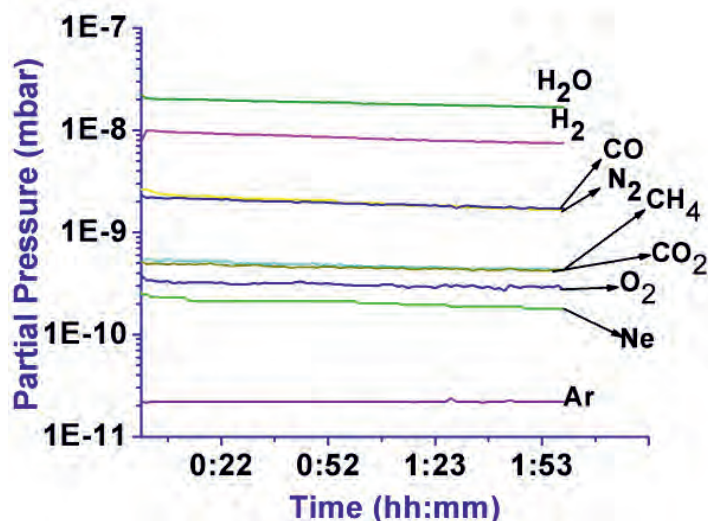

Fig. 5: Spectrum of partial pressures inside FXR tube after baking

Just before isolation of the FXR tube from the TMP pumping station, except partial pressure of water vapour and hydrogen, partial pressure of other residual gases were in the order of 10^{-9} mbar. The higher partial pressure of water vapour and hydrogen is due to the presence of PEEK inside the FXR tube. However the NEG is efficient to pump hydrogen and water vapour [3] efficiently.

b. X-ray Generation

Detail specification of pulse power unit with pulsar and power supply that was used for X-ray generation is described in [2]. The high voltage to the anode was applied through one high voltage feedthrough, co-axially mounted inside PEEK and electrically connected to the anode holder. Pulsed current was measured by one current viewing resistor connected at the input end of the FXR tube. X-ray with pulse width of 20 ns was generated by 11 kA of current when the electrodes were charged with pulsed voltage of

Table-I: Operational Parameters of FXR tube

Shot . No.	Interval between shots (minutes)	Base pressure (mbar)	Operating voltage (kV)	X-ray dose at 50 cm from X-ray window (mrad)
1	0	5.8×10^{-7}	315	30
2	2	5.0×10^{-7}	315	30
3	2	5.0×10^{-7}	315	30
4	2	5.1×10^{-7}	315	30
5	2	5.3×10^{-7}	315	30

315 kV. Dose of the X-ray was measured by ion chamber dosimeter. The angular dose of the X-ray measured at a distance of 50 cm is shown in **Fig.6**. Minimum dose at either side of 60^0 angles is due to the attenuation of X-ray at thick stainless steel end flange. At 1 m axial distance from the X-ray window, the dose was 10 mrad.

c. Vacuum Stability during Operation

Evolution of pressure inside the tube was observed for few numbers of shots, where experiments were carried out in an interval of 2 minutes.

Experiment was started with a base pressure of 5.8×10^{-7} mbar. During X-ray generation, pressure was increased to the order of 10^{-5} mbar and improved to the order of 10^{-7} mbar within 2 minutes. The increase in the pressure during X-ray generation is attributed to two different processes; electrons induced desorption of gases from the electrode surface and photon induced desorption of gases from the tube wall. **Table-I** shows the pressure value in-between shots with other operational parameters for 5 consecutive shots.

d. Radiography

Flash X-ray radiography of an epoxy filled copper coil was tested. The object was placed axially 1 m from the X-ray window. X-ray was generated with 315 kV operating voltage between the electrodes and X-ray dose at the test piece was 10 mrad. The image was captured by CR white image plate and read by computed radiography system.

Conclusion

In conclusion, one sealed off FXR tube is developed that could produce X-ray dose of 10 mrad at 1 m distance from the X-ray window which works for multiple shots in a small interval of time. This tube could be operated for up to 450 kV, which would be achieved in future endeavors.
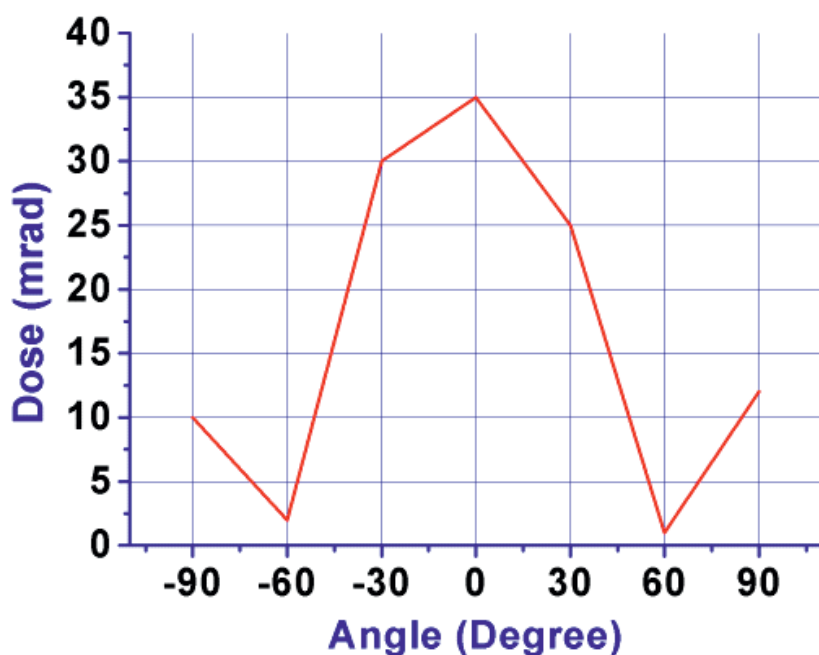
Fig.6: Angular dose distribution of X-ray.
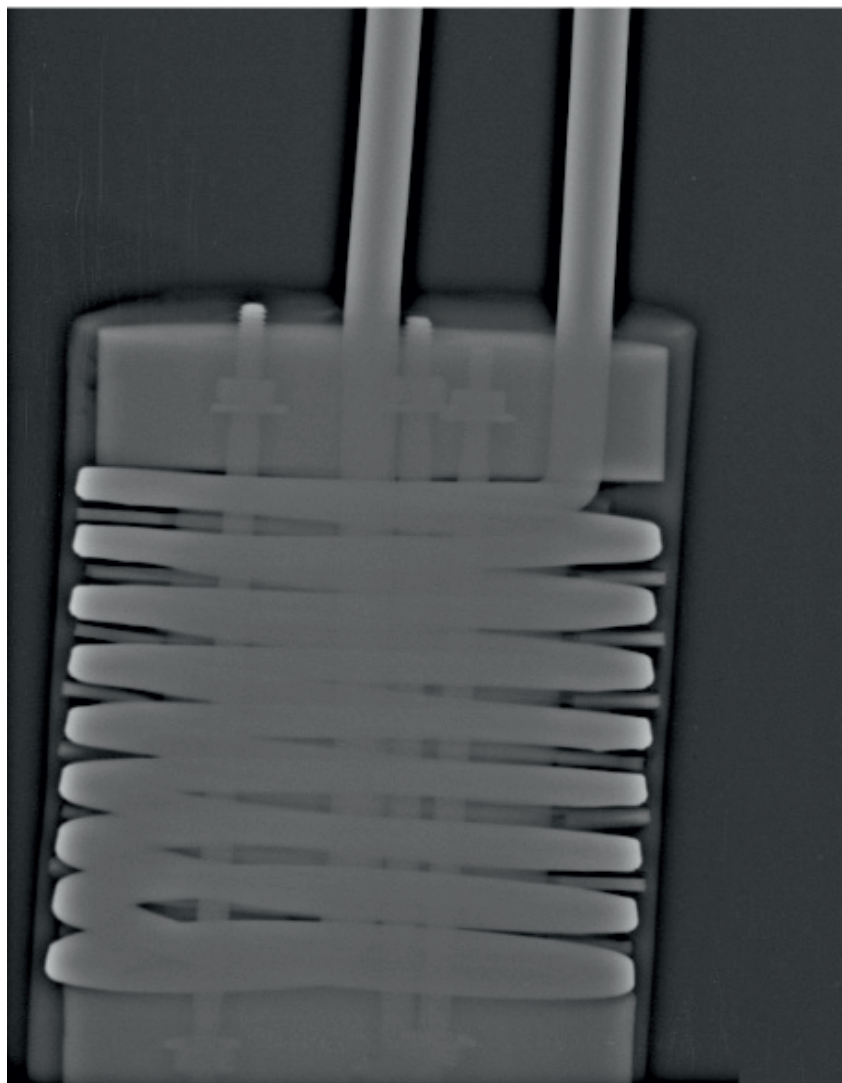
Fig.7: Radiography using sealed FXR tube at 1 m distance from the window.

Corresponding author and email:

Dr. Basanta Kumar Das
(basanta@barc.gov.in)

References

1. Ritu Agrawal, Archana Sharma and A.M. Shaikh "A Flash X-Ray System Based on Flat Pulse Marx Generator and an industrial pinch diode for Radiographic applications" Proceedings of 25th National Seminar & International Exhibition on "NDE – **2015**" Article no.-19

2. P. Banerjee et. al., "Installation and Commissioning Of Scandiflash – 450 Flash X-Ray Generator at BARC, Visakhapatnam" BARC/**2014**/E/006

3. P. Chiggiato "Production of Extreme High Vacuum with Non Evaporable Getters" Physica Scripta, T71 (**1997**) 9-13

Development of Electrical Resistance based Hull Drying Furnace for Stainless Steel Hulls of Fast Reactor Fuel Cycle Facility

Kiran T. Badgujar, R. Srinath, Kunjman Singh, K. V. Ravi
Nuclear Recycle Board, Bhabha Atomic Research Centre, Mumbai- 400085

Abstract

The Fast Reactor Fuel Cycle Facility (FRFCF) is being constructed at Kalpakkam to close the fuel cycle of Fast Breeder Reactors (FBR). The Hulls generated during reprocessing of spent fuels occupy a substantial storage at the Near Surface Storage & Disposal Facility (NSSDF) and Deep Geological Repository; thereby necessitating their volumetric reduction. Consequently, Hull Conditioning facility, to effect volumetric reduction, forms part of all upcoming waste management plants catering to high throughput reprocessing plants. Conditioning of hulls is planned to be carried out in three stages. In the first stage, the entire hull drum containing hulls will be dried to remove the residual aqueous content retained during dissolution. This is followed by the second stage which involves, hulls contained in a hull drum to be batched into smaller cans to facilitate the third stage, wherein the Cans filled with hulls are compacted in a Hydraulic Super Compactor. Elimination of aqueous content in the first stage, not only helps in avoiding any undue contamination spread during various stages of conditioning, but also reduces the susceptibility of hulls and canisters to undergo corrosion.

A first-of-its-kind prototype Electrical Resistance based Hull Drying Furnace has been designed, developed and successfully demonstrated for drying of Stainless steels hulls (501kg). This paper describes the design philosophy, constructional features, remote handling features and performance of furnace during the trials.

Keywords: Furnace, drying, batching, compaction, hull, reprocessing, waste management, dissolution

Introduction

The upcoming integrated Fast Reactor Fuel Cycle Facility (FRFCF) at Kalpakkam caters to the entire fuel cycle requirements of the Prototype Fast Breeder Reactor (PFBR). Waste Management Plant (WMP) is mandated to serve the overall waste management needs of the FRFCF including the in-house generated wastes. Hitherto, the hull wastes after being housed in storage canisters are being stored in the Tile Holes at the Near Surface Storage and Disposal Facility (NSSDF) for interim storage until further treatment before the long term storage at the Geological Repository. Hulls impose a burden on the definite storage space available at the NSSDF and Geological Repository. Hulls being hollow cut pieces provide immense scope for volumetric reduction thereby minimizing the long term storage space requirements. Consequently, compaction of hulls has been envisaged to effect volumetric reduction.

Drying is used to eliminate the residual aqueous content present in the hulls. It is necessitated to address the vulnerability of hulls to undergo corrosion during storage [1]. Drying of hulls also restricts the contamination spread on account of dripping of loose aqueous content sticking to the hulls during the course of batching operation and compaction. Drying of the entire hull drum containing 400 litres of hulls is followed with batching operation wherein the hulls housed in the hull drum are batched into hull Cans of 60-70 litres capacity for ease of compaction. Compaction of hulls is accomplished by means of a Hydraulic Super Compactor [2].

A prototype Pit Type Electrical Resistance Furnace (1:1 scale) has been developed & demonstrated to carry out drying of stainless steel hulls. The present work broadly involved selection of drying technique, feasibility trials, design, fabrication, assembly and mock up trials on the furnace. Hull Drying Furnace installed at Test Facility, Kalpakkam, is shown in the **Fig. 1**. Mock-up trials were conducted for two different temperatures viz. 350°C and 550°C. Temperature at six different locations across the length of
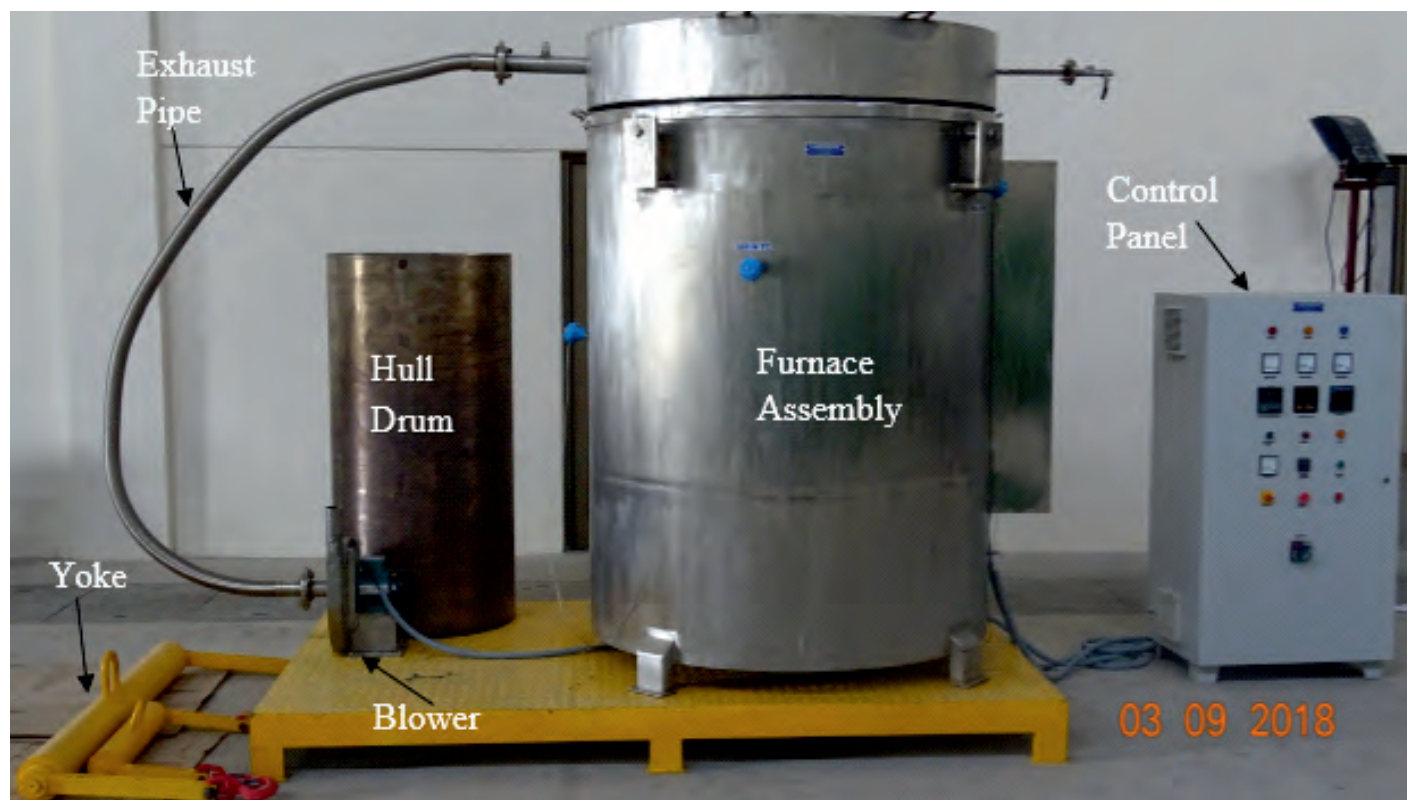
Fig.1 Hull Drying Furnace installed at Test Facility, Kalpakkam

the furnace, relative humidity and temperature of the exhaust air were monitored and recorded during the course of trials. Time history of monitored parameters was recorded for subsequent assessment and inference.

Selection of Drying Technique

Broadly, two different methods can be adopted for drying viz. Direct heating and Indirect heating. Direct heating involves injection of hot dry air in a drum housing wet hulls thereby bringing the air to come into physical contact with the wet hulls to cause evaporation. C.K. Chakrabarti et al. experimentally investigated the performance of a Hull Drying unit using hot dry air [3]. It was reported that for a perforated bottom Can (Diameter 326 mm, Height 700 mm), containing 21 kg of hulls with a retained water content of 1 kg, the drying time was found to be 86 minutes corresponding to an air temperature of 115 °C and air flow

rate of 1000 SLPM. Indirect heating employs a furnace to transfer the requisite sensible heat and latent heat of vaporization to the wet hulls, to achieve drying. Indirect heating by means of Electrical Resistance based Furnace has been chosen over Direct Heating, owing to lesser volume of secondary off-gas generation, amenability for use of non-perforated Hull Can/Hull drum, reduction in alpha contamination of off-gas treatment system, high through-put and simplicity in operation.

Feasibility Study on Scaled down model

Feasibility tests were conducted on a small scale Electrical Resistance Furnace (Experimental set up) shown in **Fig.2** to assess the efficacy of indirect heating technique in drying the hulls. **Table 1** gives the test conditions and **Fig. 3** depicts the change in surface temperature of drum housing hulls and change in temperature of exhaust air with time.

It was observed that the exhaust air temperature increased with time, it remained constant for certain duration, then decreased and finally leveled off thereby indicating the attainment of thermal equilibrium. Total drying time observed was 140 minutes. The drying of hulls was verified by visual examination as well as by measurement of weight of the hull drum before and after drying.

Mock-Up Trials on Prototype Furnace

Based on the experience gained from the feasibility study, a prototype Electrical Resistance furnace has been developed. Salient features of the furnace are outlined in the **Table 2**.

Constructional Details

The constructional detail of the furnace is shown in **Fig.4**. The innermost drum containing the wet hulls is referred to as Hull drum. The hull drum is housed in a cylindrical drum called Susceptor, which acts as a

Fig.2 Experimental setup for Feasibility of hull drying using electrical resistance heating furnace
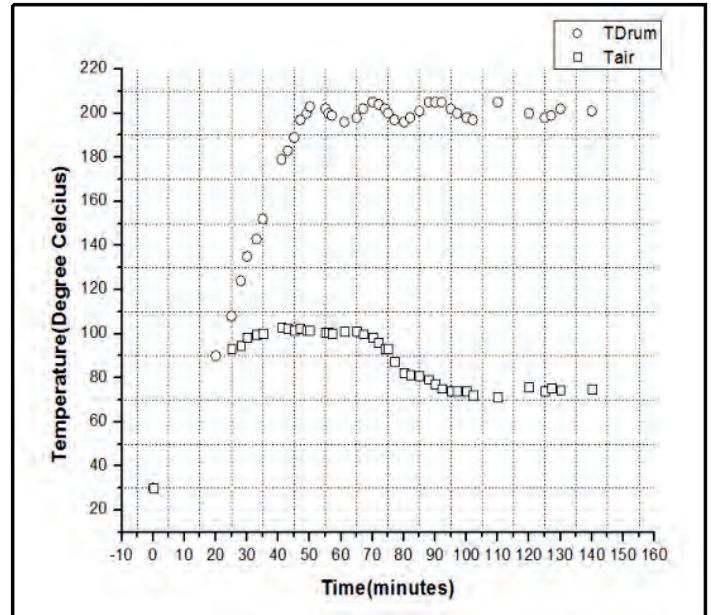

Fig.3 Variation of exhaust air temperature with time and with surface temperature of hull drum

barrier between the Hull drum and Heating element. Susceptor is provided with convolutions to account for the axial thermal expansion arising due to elevated temperatures. Surrounding the Susceptor circumferentially is the Heating element which forms the heat source. Insulating material is placed around the outside surface of heating element to minimize the heat loss. Refractory bricks form the base of the furnace. External Casing along with structural members acts as the skeleton of the furnace.

Special Features

Following features have been incorporated in the design of furnace for its suitability of operation in the radioactive hot cell

• Sealed stainless steel construction of furnace ensures easy decontamination of all the surfaces for disposal

• Hinged lid design to minimize space requirements in the hot cell

• Ease in remote removability of furnace from the hot cell

Table 1- Feasibility Test conditions

Size of simulated hulls	Outside Diameter	6.6 mm
	Thickness	0.45 mm
	Length	30mm
Size of hull drum	Outside Diameter	350 mm
	Thickness	5 mm
	Height	500 mm
Set - point temperature		200 °C
Mass of hulls		5 kg
Mass of water		0.5 kg
Power Input		2 kW

Table 2 Salient features of Electrical Resistance based Hull drying Furnace

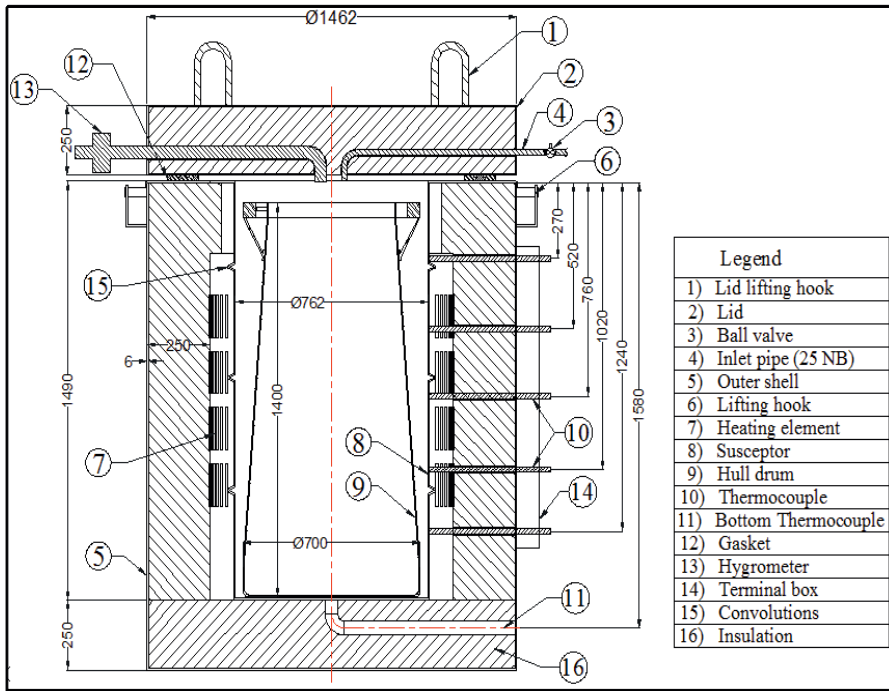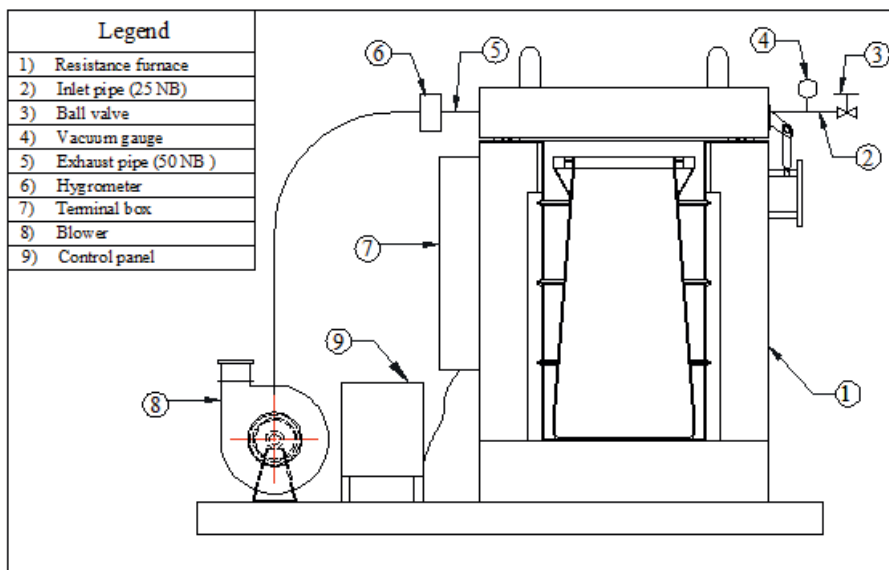| Capacity		36 kW
Heating element	Material	Nikrothal 80/20
	Configuration	Rod-Over-Bend
Insulation		Ceramic Fibre & Refractory bricks
Material of construction		SS 304 L
Control system	Furnace Control	Program Controller
	Safety Controller	PID
Thermocouples		'k' type
Exhaust blower		100 CMH & 50 mm of WC
Lid gasket		Silicon

Fig.4 Constructional details of the Furnace

Legend	
1)	Lid lifting hook
2)	Lid
3)	Ball valve
4)	Inlet pipe (25 NB)
5)	Outer shell
6)	Lifting hook
7)	Heating element
8)	Susceptor
9)	Hull drum
10)	Thermocouple
11)	Bottom Thermocouple
12)	Gasket
13)	Hygrometer
14)	Terminal box
15)	Convolutions
16)	Insulation

Fig. 6 Location of Thermocouples & Hygrometer

Legend	
1)	Resistance furnace
2)	Inlet pipe (25 NB)
3)	Ball valve
4)	Vacuum gauge
5)	Exhaust pipe (50 NB)
6)	Hygrometer
7)	Terminal box
8)	Blower
9)	Control panel

Fig.5 Experimental set-up for Mock-up trials

• Ease in the replacement of thermocouples and gasket using manipulators

Experimental set-up

The experimental set-up broadly comprises of furnace, blower, control panel, vacuum gauge, thermocouples and a hygrometer. Schematic of the experimental set-up is shown in **Fig.5**. The water vapors emanating from the furnace are sucked in by the blower through a 50 NB exhaust pipe.

Hygrometer mounted on the exhaust pipe was used to measure the relative humidity and temperature of the exhaust air. An inlet pipe has been provided to bleed air into the furnace. Vacuum gauge mounted on the inlet pipe was used to monitor the negative pressure inside the furnace. Temperature measurements were carried out at six different locations using thermocouples viz. T_{SC}, T_{FC}, T_1, T_2, T_3 and T_4 as depicted in the **Fig.6**. Power supply to the furnace was

controlled by means of Program Controller mounted on the control panel. A Safety controller (PID) was used to limit the temperature of furnace beyond a set upper limit.

Experimental Procedure

Firstly, a perforated SS drum (275 mm diameter, 380 mm length) filled with 30 kg hulls was drenched in water and allowed to soak in to estimate the retention of water. Retention of water was measured to be 900 gm for 30 kg Hulls. The quantity of water retained with 30 kg hulls was extrapolated for 501 kg of hulls. Accordingly, 15 kg of water for 501 kg of hulls was added to the hull drum manually as shown in **Fig. 7** . The hull drum filled with wet hulls being loaded into the furnace is shown in **Fig.8**. This was followed by fixing of a Set-point temperature with the Program Controller which draws input from the thermocouple T_{FC}. Set-point temperature is the temperature at which the Furnace is meant to be operated. The percentage of power supplied to the furnace from the control panel was also fixed. Soaking time for the trial was set with the program controller. An upper limit for the temperature was fixed

Fig.7 Addition of water in hull drum

Fig.8 Loading of hull drum in furnace

with the Safety controller, which draws input from the T_{SC} Thermocouple. As the power supply was turned on, temperature and relative humidity readings were systematically noted at fixed intervals of time to generate the time-history of parameters being monitored.

Observations, Results and Discussions

Two sets of Trials were carried out for a set-point temperature of 350˚C and 550˚C with the test conditions outlined in **Table 4** & **Table 5** respectively. The overall trend of temperature versus time is shown in **Fig.9**. The rate of rise in temperature of $T_{SC}, T_{FC}, T_1, T_2 \& T_3$ was high till the set-point temperature (Soaking Temperature) of 350˚C. Thermocouple T_4 located at the bottom of the hull drum registered a sluggish rate of temperature rise with the maximum being 69˚C after four and half hours of soaking time.

This is attributed to the existence of thermal stratification with the lowest temperature being observed at the bottom of the hull drum. The rate of temperature rise of exhaust air was also observed to be steady reaching about 82˚C after the said soaking duration. Relative humidity of exhaust air was found to be steadily decreasing with time. The relative humidity eventually saturated at 8% and the furnace was switched off to allow it to cool naturally with the exhaust blower kept on. Weight of the

Trial -1 (Set Point Temp. 350 ˚c)

Table 4 - Test Conditions		
Size of simulated hulls	Outside Diameter	6.6 mm
	Thickness	0.45 mm
	Length	30mm
Set-point temperature		350 °c
Mass of hulls		501 kg
Mass of water		15 kg
Power Input		18 kW
Upper Limit of Temperature in Tsc		600 °c
Ramping time		2 hrs
Soaking time		4 hrs 20min

Fig.9 Variation of parameters with time during Trial-1

Trial-2 (Set Point Temp. 550 °c)

Table 5 - Test Conditions

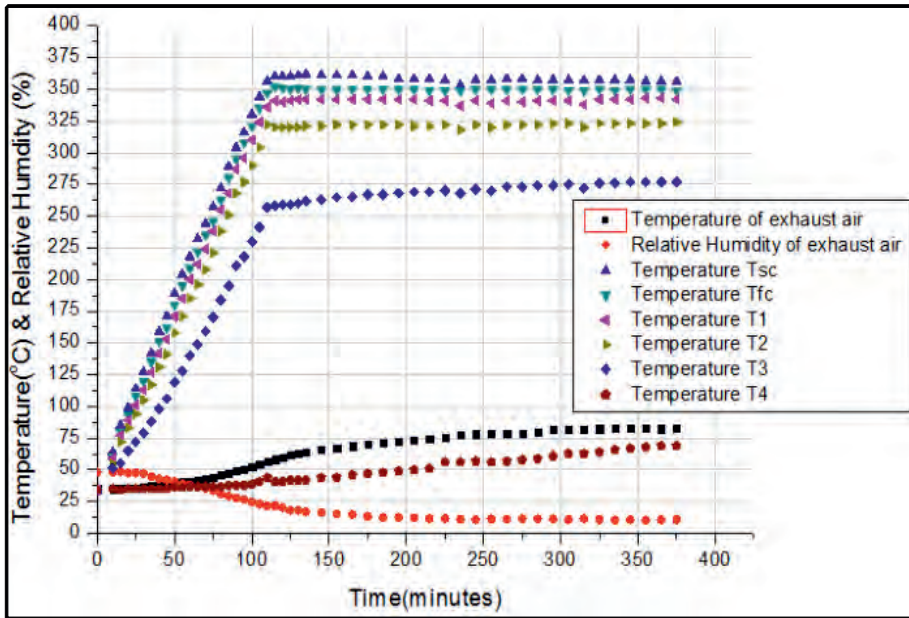| Size of simulated hulls	Outside Diameter	6.6 mm
	Thickness	0.45 mm
	Length	30mm
Set-point temperature		550 °c
Mass of hulls		501 kg
Mass of water		15 kg
Power Input		18 kW
Upper Limit of Temperature in T_{SC}		600 °c
Ramping time		4 hrs
Soaking time		3 hrs 10min

Fig. 10 Variation of parameters with time during Trial-2

hull drum was measured post the soaking operation. It was found that out of 15 kg of water content in the hull drum prior to drying, 12.4 kg of water was removed. The presence of 2.6 kg of water after drying operation at 350˚C is indicative of need for higher set-point temperature and drying time to ensure complete drying of hulls. The removal of water content is by virtue of both the effects of evaporation and boiling. Boiling aids in the removal of water in the regions closer to the bottom of the hull drum where the circulation of air is not very dominant and the temperature of contents are typically lower than the upper regions of the hull drum.

The general trend of temperature versus time curves across the length of susceptor remained similar for Trial-2 as well, as depicted in the Fig.10. The drying time (Ramping time + Soaking time) was maintained higher to ensure complete drying. The highest temperature measured by T4 thermocouple at the end of soaking period was 152˚C. This is indicative of the temperature of the contents of the hull drum being higher than the Saturation temperature of water (100 ˚C at 1 atm). This ensures that the water sticking to the hulls present in the bottom region of the hull drum undergoes boiling. Temperature and Relative humidity of exhaust air registered at the hygrometer was 152 ˚C and 1.2% respectively. As the relative humidity saturated at 1%, the furnace was switched off to allow it to cool naturally with exhaust blower kept on. Weight of the contents of hull drum (hulls and water) when measured post the soaking operation, was found to be equal to the weight of the hulls thereby indicating the absence of any residual water content.

Visual examination was also carried out to confirm the drying of hulls.

Conclusion

Complete drying of hulls for a set-point temperature of 550˚C establishes the suitability of Electrical Resistance based furnace for the hull drying application. The drying of hulls is on account of evaporation and boiling. Evaporation aided by high temperature of air and convection takes away the bulk of water content. Boiling helps to remove the residual water content at the centre and bottom regions of the hull drum where the air circulation is not very prominent. Complete drying in case of Trial-2 was ensured because of the bottom of the hull drum being at a temperature greater than 100˚C for close to five hours during the drying period. The developed hull drying furnace establishes its suitability for plant scale operations owing to its simplicity in operation, ease of remote maintenance and operation, ease of decontamination and longevity.

Corresponding author and email: Shri Kiran T. Badgujar (kirantb@barc.gov.in)

Acknowledgements

References

1. F. Chotin, Ph. Pinson, COGEMA, "The Atelier De Compactage Des Coques (ACC) Facility: The R&D Programme", IAEA-SM-357/30

2. A.A. Manole, P.P. Karkhanis, Kailash Agarwal, Shekhar Basu, "Development of Hull Compaction System for Nuclear Recycle Facility", BARC Newsletter, Issue no. 334, **(2013)**: 32-37

3. C.K Chakrabarti, K.M Singh, K. Banerjee, S Bowmick, K. T Shenoy, "Evaluation of Performance Characteristics of a Hull Drying Unit". BARC Newsletter, May- June **2015**.

Development of Biodegradable Film from Fish Processing Waste: An Environment Friendly Initiative

R.K. Gautam, A.S. Kakatkar, P.K. Mishra, V. Kumar and S. Chatterjee

Seafood Technology Group, Food Technology Division
Bhabha Atomic Research Centre, Trombay, Mumbai- 400 085

Abstract

Biodegradable films were developed using fish protein gel dispersion prepared from fish processing waste with incorporation of antioxidants (BHT & Ascorbic acid). The thickness of various films namely FG (fish gel), FGS (fish gel with starch), FGB (fish gel with BHT) and FGA (fish gel with ascorbic acid) ranged between 0.08 to 0.09 mm. The physical, mechanical, barrier and colour properties of films showed no significant variations during 12 month storage at ambient temperature. However, film with combination of ascorbic acid and fish gel (FGA) showed a better tensile strength (1.23 MPa), higher elongation at break point (127.97%) and lower water solubility (10.57%) as compared to FG, FGS and FGB. These film characteristics were comparable to other biodegradable films. The study indicates feasibility of effective utilization of fish processing waste for development of suitable packaging material. The utilization of fish waste may help in significant reduction in its disposal cost generating additional revenue and thus providing cleaner environment.

Keywords: Fish waste, Protein gel dispersion, Antioxidants, Bio-degradable, Packaging

Introduction

Research in biodegradable polymeric films for food packaging is witnessing significant interest as an alternative approach to tackle widespread use of plastic and disposal of plastic materials. A biodegradable film that is eco-friendly, non-toxic and gifted with physical and chemical properties of a synthetic polymeric film is the need of the hour. Natural bio-polymers like protein, polysaccharides, lipids or their combination can be utilised for preparation of biodegradable films (Tongnuanchan et al., **2012**). Amongst these, proteins have been extensively studied because of their relative abundance, film-forming ability and nutritional qualities. Generally, protein based films provide mechanical stability whereas polysaccharides are used to control oxygen and transmission of various other gases. As the protein-based films degrade, they provide a source of nitrogen acting as fertilizer, an additional benefit over other non protein-based films. These films act as selective barrier against the transmission of gases, vapours, and solutes which improves food quality, extend shelf life and provide physical protection (Zhong and Xia, **2007**).

Processing of fish generates enormous amounts of waste material, such as fish heads, skin etc. For example in case of fish fillets, 75% of the total fish weight accounts for fish waste. This fish processing waste can be useful in development of biodegradable film. The utilization of fish waste helps to generate additional revenue, with safe and low cost of disposal, providing a cleaner environment (Mathew, **2014**). Few studies have been reported on fish protein based biodegradable films which can enhance the shelf life of fresh and frozen foods (Aristippos and Curtis, **1990**).

Aim of the present work was to develop a biodegradable film using fish processing waste and discards and to characterize their mechanical and barrier properties, comparison of changes in mechanical and barrier properties on incorporation of soluble starch and antioxidants like Butylated hydroxy toluene (BHT) and ascorbic acid during storage at ambient temperature.

Development of biodegradable film & its stability during storage

Composition of fish protein gel & its source

Fish protein dispersion was obtained through acid gelation of myofibrillar proteins isolated from fish processing waste. Myosin is the major structural protein of vertebrate muscle including fish muscle which plays an important role in the gelation and

emulsification of muscle based food (Venugopal, **1997**).

Physical & Mechanical properties

Various biodegradable films **Fig. 1** were developed using fish protein gel dispersion (Kakatkar, **2004**) prepared from fish processing waste with incorporation of antioxidants (BHT& Ascorbic acid) by casting method as described by Rao etal. (**2010**). Thickness of the FG (fish gel), FGS (fish gel with starch), FGB (fish gel with BHT) and FGA (fish gel with ascorbic acid) were 0.08 ± 0.01, 0.09 ± 0.01, 0.08 ± 0.01, and 0.08 ± 0.01 mm respectively. Evidently, there was no significant difference in thickness of the films. The thickness of the films was comparable to earlier reports with average thickness of the films from fish proteins ranging from 0.08 to 0.13 mm. (Ninan, **2010**).

Tensile strength (TS) and elongation at break (ELB) was measured according to ASTM method D882-00 (ASTM, 2001). Mean TS of FG, FGS, FGB and FGA ranged from 0.99 ± 0.04 to 1.44 ± 0.06MPa **Fig. 2a** . Mean ELB of FG, FGS, FGB and FGA ranged 93.67 ± 1.0 to 127.97 ± 1.07 (%) respectively (**Fig. 2b**). FGA had maximum ELB (127.97%), and TS (1.23MPa), While FGS resulted in highest TS (1.44MPa), and ELB (107.27%). The mechanical properties showed that FGA films were better than FGS, FGB and FG. There were no significant changes in physical properties of films during storage at ambient temperature over a period of 12 months. Similar edible and biodegradable packaging films based on fish myofibrillar proteins have shown TS of 17.1 MPa, ELB of 22.7%, at a thickness of 0.034 mm (Cuq et al., **1995**). Kaewprachu and Rawdkuen (**2014**) showed that
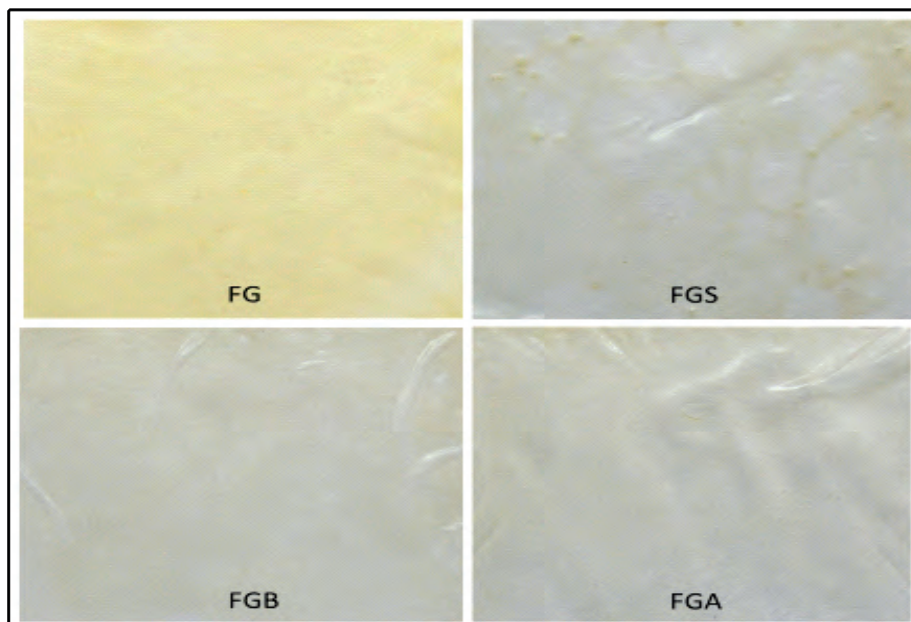
Fig.1: Various biodegradable films developed from fish waste

biodegradable films from giant catfish skin gelatine showed a higher TS (26.42 MPa) and ELB (128.25%). A higher TS of 5.86 MPa and 123.5 % of ELB had been reported from edible films based on Alaska Pollack (Shiku et al., 2004). Variation in the data could be due to compositional differences and the procedure employed for film preparation. FGA films showed better mechanical properties with higher tensile strength and elasticity than other films over a period of 12 months.

Barrier properties

Barrier properties of a polymer are crucial to product-package shelf-life. The specific barrier requirement of a package system depends upon the food characteristics and the intended end-use applications (Siracusa, **2012**). Water vapour transmission rate was done based on ASTM E96/E96M-05 method. WVTR of the films were comparable and it ranged from 0.381 ± 0.0072 to 0.4071 ± 0.0069 g/cm^2/day (**Fig. 2c**) with no significance variation in means. The WVTR of films remained unaffected during storage for 12 month at room temperature. WVTR of fish films were comparable and found to be lower than other similar films like gelatin-starch film (1.08 ± 0.01 g/cm^2/day), albumin-starch film (0.938 ± 0.01 g/cm^2/day), casein-starch film (0.892 ± 0.01 g/cm^2/day) as reported by Jagannath et al., (**2003**) and surimi based edible film (1.69 ± 0.06 gm^{-1}s^{-1}Pa^{-1}) as described by Shiku et al., (**2004**).

Films have shown varying degree of oxygen permeability in terms of oxygen transmission rate (OTR), with FG resulting as impermeable to oxygen, while FGA and FGB were oxygen permeable in order of 153 ± 3.6 ml/m^{2}xday, and 999 ± 3.7 ml/m^{2}x day respectively (**Fig. 2d**). Oxygen permeability of FGS film could not be measured as it became brittle and tore off while measurement. Fish films showed higher rate of oxygen transmission and compared with other reported films like, Cellulose acetate phthalate film (CAP film) and Gluten film, which showed lower oxygen permeability of 22.21 ± 1.23 % ml/m^{2}xday and 41.02 ± 0.86 % ml/m^{2}xday respectively (Falchouri et

al., **2004**). Improving oxygen barrier performance of a film helps as oxygen promotes degradation of food by oxidation and thus affects organoleptic properties of food (Siracusa, **2012**).

Water solubility of film

Water solubility of FG, FGA and FGB was 13.97 ± 1.22 %, 10.57 ± 1.23 % and 11.9 ± 1.24 % respectively, while FGS was more water soluble with 20.79 ± 1.17 % solubility (**Fig. 2e**). Cellulose acetate phthalate film (CAP film) and gluten film have 100 % and 22.7 ± 4.10 % water solubility (Falchouri et al., **2004**).

Colour change

Colour of the film was measured as per method described by Pires 2011 using Minolta CM-3600d Spectrophotometer (Konica Minolta Sensing, Inc, Osaka, Japan). The whole visible spectrum (360 to 780 nm) was recorded with Δλ = 10 nm and considering illuminant D65 and 10˚ observer as references.

The CIELAB parameters, L*(lightness), the chromaticness coordinates, a* (+red to –green component), and b* (+yellow to –blue component) were analysed by JAYPAK software (Quality Control System, Version 1.2). Means of hunter L*a*, and b* values were determined after taking average of 3 colour value parameters (each in triplicates)across each film, and the difference in colour components during storage were analysed statistically by using one-way analysis of variance (ANOVA).Changes in colour components for samples analysed during storage at ambient temperature **Fig. 3.** L* values [lightness or clarity, which ranged from 0 (black) to 100 (colourless)] of the samples did not change significantly (P < 0.05) during storage over a period of 12 months. There was a slight reduction in a* values [chromatic co-ordinates, which ranged from red (+) to green (-)] towards greenness without any significant change (P < 0.05). However, there was significant difference in b* values [chromatic co-ordinates, which ranged from yellow (+) to blue (-)]of the FG and FGS films. Whereas, b* values of the FGB
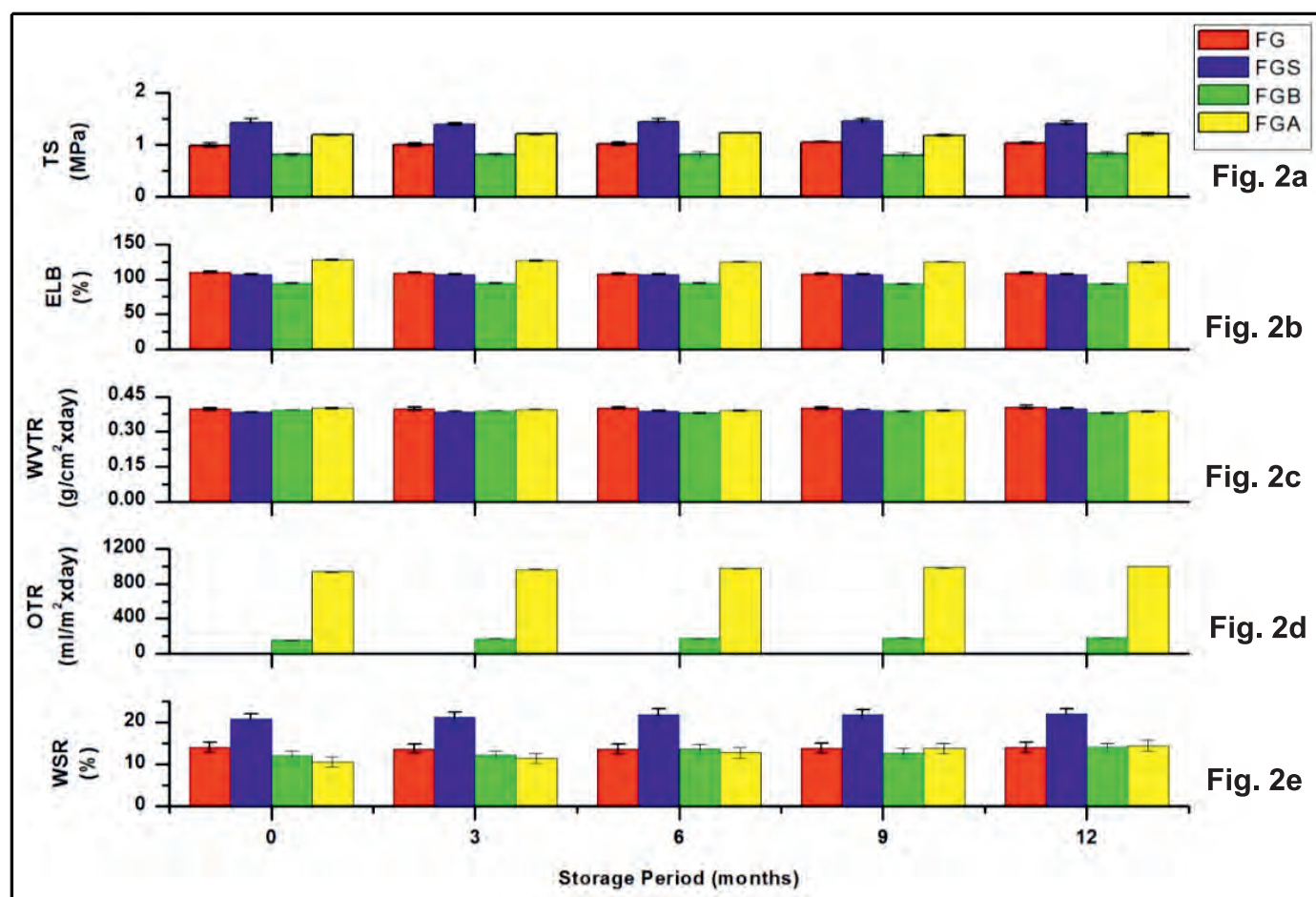

Fig. 2: Mechanical [Tensile Strength (TS), Elongation at Break (ELB)]; Barrier (Water Vapour Transmission Rate (WVTR), Oxygen Transmission Rate (OTR)] properties and Water Solubility Rate (WSR) of biodegradable films & their changes during 12 month of storage period. The values shown above are mean ± SD of three independent experiments, each carried out in triplicates.

and FGA films changed insignificantly (P < 0.05). Films had shown a slight yellowish discoloration, which may be due to non-enzymatic browning reactions between protein components.

Conclusion

Combination of fish protein, starch and antioxidants lead to successful development of clear, flexible biodegradable films. The film with combination of ascorbic acid and fish gel (FGA) showed a better tensile strength along with higher elongation at break point as compared to FG, FGS and FGB. Thus, inclusion of ascorbic acid as antioxidant has provided better protein-based biodegradable packaging film. The study shows effective use of fish protein for preparation of environment friendly biodegradable films, which can be used in food packaging industry.

Corresponding author and email:
Smt. Chatterjee S (suchanc@barc.gov.in)

References

1. G. Aristippos, L.W. Curtis. 1990. Edible Films and Coatings from Wheat and Corn proteins. Food Technol. 44(10): 63-69.

2. ASTM D 882-00. **2001**. Standard test method for tensile properties of thin plastic sheeting. Annual book of ASTM standards. Philadelphia PA: American Society for Testing and Materials.

3. ASTM E 96-95. **2005**. Standard test methods for Water Vapor Transmission of Materials. Annual book of ASTM standards. Philadelphia PA: American Society for Testing and Materials.

4. B. Cuq, N. Gontard, J.L. Cuq and S. Guilbert. 1995. Edible packaging films based on fish myofibrillar
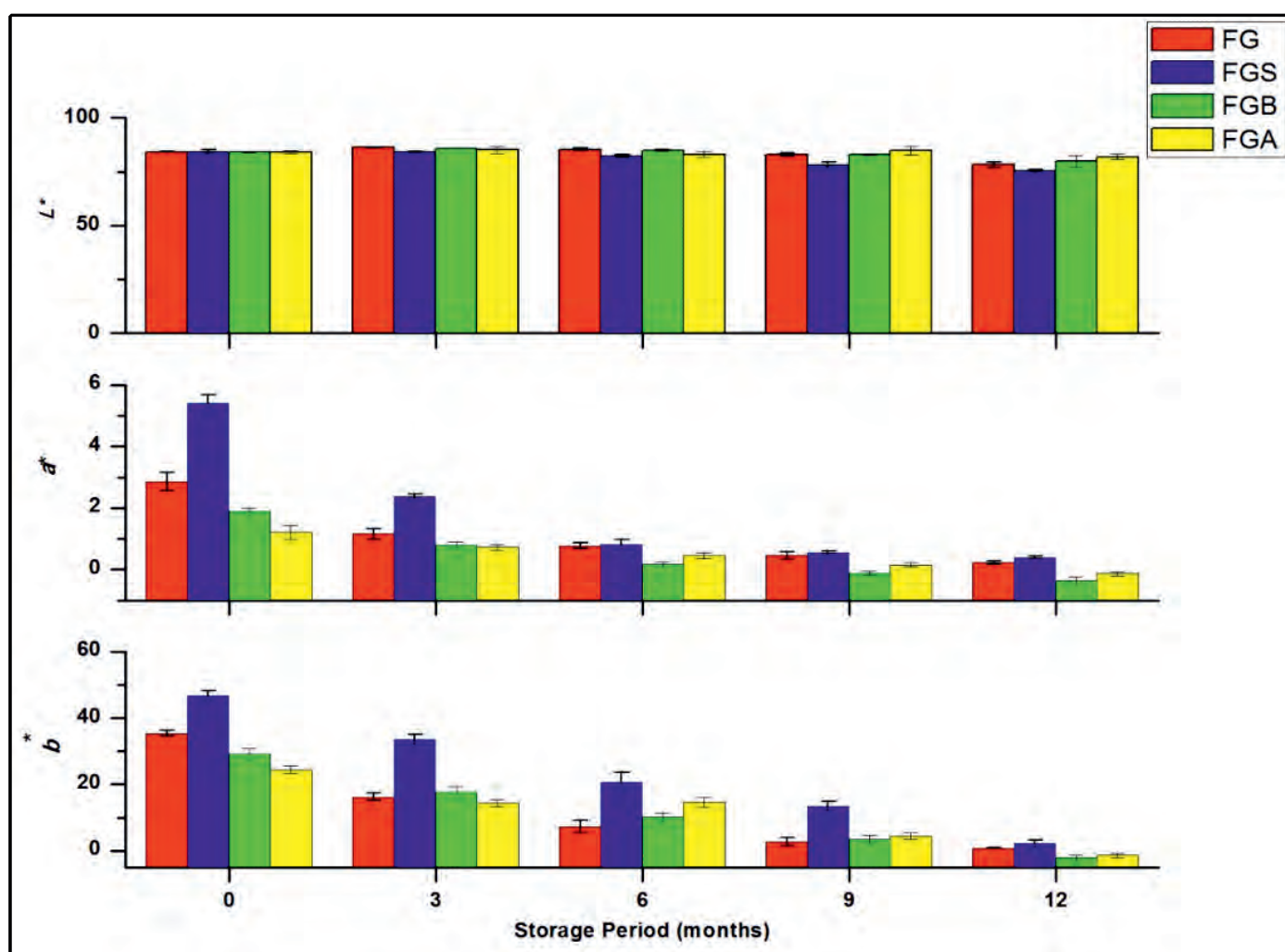
Fig. 3: Changes in colour (L⁺, a⁺, b⁺ - values) of the films during storage period. The results shown are mean ± SD of three independent experiments, each carried out in triplicates. L⁺ values - lightness or clarity, which ranged from 0 (black) to 100 (colourless); a⁺ values - chromatic co-ordinates, which ranged from red (+) to green (-); b⁺ values - chromatic co-ordinates, which ranged from yellow (+) to blue (-).

proteins: Formulation and functional properties. J. Food Sci. 60, 1369-74.

5. F.M. Falchouri, P.S.Tanada-Palmu and C.R.F. Grosso. **2004**. Characterization of composite biofilms of wheat-gluten and cellulose acetate phthalate. Braz. J Chem. Eng. 21(2): 261-64.

6. J.H. Jagannath, C. Nanjappa, D.K. Das Gupta, & A.S. Bawa. **2003**. Mechanical and barrier properties of edible starch-protein based films. J. Appl. Polym. Sci. 88(1): 64-71.

7. P. Kaewprachu and S. Rawdkuen. **2014**. Mechanical and physico-chemical properties of biodegradable protein-based films: A comparative study. Food Appl. Biosci. J. 2(1): 15-30.

8. A. Kakatkar, S.V. Sherekar and V. Venugopal. **2004**. Fish Protein dispersion as a coating to prevent quality loss in processed fishery products. Fish Technol. 41, 29-36.

9. P.T. Mathew. **2014**. Fishery waste management- problems and prospects. In: Recent advances in the development of nutraceuticals, health foods and fish feed from fish and shellfish processing discard (Eds.) A. A. Zynudeen, J. Bindu, G. Ninan, C.O. Mohan, & R. Venkateshwarlu. ICAR-Central Institute of Fisheries Technology, Cochin, Kerala, India. Pp. 11-26.

10. G. Ninan, J. Joseph, and Z. Abubacker. **2010**. Physical, mechanical, and barrier properties of carp and mammalian skin gelatine films. J. Food Sci. 75(9): E620-E626.

11. C. Pires, C. Ramos, G. Teixeeira, I. Batista, R. Mendes, L. Nunes and A. Marques. **2011**. Characterization of biodegradable films prepared with hake protein and thyme oil. J. Food Eng., 105, 422-428.

12. M.S. Rao, S.R. Kanatt, S.P. Chawla and A. Sharma. **2010**. Chitosan and Guar gum composite films: preparation, physical, mechanical and microbial properties. Carbohydr. Polym. 82, 1243-7.

13.Y. Shiku, P.Y. Hamaguchi, S. Benjaku, W. Visessanguan and M. Tanaka. **2004**. Effect of surimi quality on properties of edible films based on Alaska pollack. Food Chem., 86, 493-99.

14. V. Siracusa. 2012. Food packaging permeability behaviour: A report-review article. Int. J. Polym. Sci. 2012, Article ID 302029, 11 pages, https://doi.org/10.1155/2012/302029

15. P. Tongnuanchan, S. Benjakul and T. Prodpran. **2012**. Properties and antioxidant activity of fish skin gelatine film incorporated with citrus essential oils. Food Chem. 134(3): 1571-9 https://doi.org/10.1016/j.foodchem.2012.03.094

16. V. Venugopal. **1997**. Functionality and potential applications of thermostable water dispersions of fish meat. Trends Food Sci Technol, ISSN: 0924-2244, Vol: 8, Issue: 8, Page: 271-276 https://doi.org/10.1016/S0924-2244(97)01038-8

17. Q.P. Zhong, W.S. Xia. **2007**. Physiochemical properties of edible and preservative film chitosan/cassava starch/gelatine blend plasticized with glycerol. Food Technol. Biotechnol., 46: 262-9.

Production of clinical grade ^{90}Y-acetate for therapeutic applications using ultra pure ^{90}Sr recovered from PUREX HLLW

[1]Poonam Jagasia, [2]Arpit Mitra, [1]P. W. Naik, [1]R. K. Mishra, [1]K. C. Pancholi, [1]R. Kannan, [1]Amar Kumar,[3]Anilkumar S. Pillai, [1]P.S. Dhami, [1]J. S. Yadav, [2]Sharmila Banerjee, [1]C.P. Kaushik and [1]K. Agarwal

[1]Nuclear Recycle Group, BARC, Trombay, Mumbai- 400085
[2]Radiation Medicine Centre, Parel, BARC, Mumbai- 400012
[3]Radiation Safety Systems Division, BARC, Trombay, Mumbai- 400085

Abstract

High Level radioactive Liquid waste (HLLW) obtained from reprocessing of spent fuel by PUREX process is a rich source of ^{90}Sr which is a pure β- emitter and decays to ^{90}Y, a very useful radionuclide in nuclear medicine for cancer therapy. A solvent extraction based Plant is being operated in the hot cells of WIP, Trombay, for management of HLLW using indigenously synthesized solvents. The secondary streams from the Plant are being employed for the recovery of many useful radionuclides. One of the streams from this process is found ideal to recover ^{90}Sr(NO$_3$)$_2$ solution of high specific activity. In view of generating clinical grade carrier-free ^{90}Y, availability of high purity ^{90}Sr is most important requirement. In Process Control Laboratories of NRG, multi step separation processes involving solvent extraction, extraction chromatography, radiochemical precipitation and membrane based techniques have been used to purify ^{90}Sr to generate clinical grade ^{90}Y. A two-stage Supported Liquid Membrane based ^{90}Sr-^{90}Y generator system developed in-house is used for milking carrier-free ^{90}Y-acetate. Clinical grade ^{90}Y-acetate in batches of ~140-160 mCi are separated and transported to Radiation Medicine Centre, Parel, BARC for radiopharmaceutical applications. Approved transport procedure by BARC Safety Council is followed for transporting the activity from Trombay to RMC, Parel.

Introduction

Utilization of radioisotopes for diagnosis and therapy of various diseases in health care is one of the important programme of Department of Atomic Energy. Several radionuclides are produced using research reactors and particle accelerators for applications in nuclear medicine.The High Level radioactive Liquid waste (HLLW) generated during reprocessing of spent fuel by PUREX process is a rich source of many useful radionuclides viz.[137]Cs, ^{90}Sr, ^{90}Y, [106]Ru, [147]Pm, [144]Ce, [231]Pa, [237]Np, [241]Am, and [252]Cf etc. It is therefore considered as resource rather than a waste. Separation and purification of these radionuclides from such streams is extensively being explored in Nuclear Recycle Group (NRG), BARC, Trombay.

Yttrium-90, a pure β-emitter (E_{max} = 2.28MeV, $T_{1/2}$ = 64.1h), is a potential therapeutic radionuclide formed by β$^-$ decay of[90]Sr, which is available in large quantities in HLLW. On separation and purification, it can be used as a long lasting source for the generation of carrier-free [90]Y. To separate ^{90}Y from ^{90}Sr, several techniques such as extraction chromatography, electrochemical and supported liquid membrane based generator systems were studied in our laboratory at Trombay [1-6]. Among these, a two-stage supported liquid membrane (SLM) based generator system [5] is extensively pursued in our laboratories at NRG and is found to be a convenient system for milking carrier-free[90]Y.

In view of high purity carrier-free[90]Y to be used in radiopharmaceutical applications, earlier a 2-stage [90]Sr -^{90}Y generator system was proposed [5, 7]. Based on the extensive studies the generator system was found suitable in getting the purity of[90]Y with respect to [90]Sr (<10^{-6}Ci/Ci of [90]Y i.e. 10^{-4}% of total activity) as desired for clinical grade [90]Y. As per European Pharmacopeia the purity requirements with respect to α activity are more stringent (10^{-9}Ci/Ci[90]Y) as compared to[90]Sr [8].

Nuclear Recycle Group made a collective effort to separate and purify high specific activity[90]Sr from HLLW

using a multi stage solvent extraction loop at Waste Immobilization Plant (WIP), Trombay removing bulk of uranium, cesium, lanthanides and actinides. Since a single separation technique is unable to recover ^{90}Sr of desired radionuclidic purity from such waste solution containing host of minor actinides, fission products and other metallic elements, multi separation techniques *viz*. solvent extraction, ion-exchange, extraction chromatography and membrane based methods were employed for purification. The purified ^{90}Sr $(NO_3)_2$ was used to generate carrier-free ^{90}Y by employing two-stage Supported Liquid Membrane (SLM) generator. Various steps employed during separation, purification and assaying its quality to make it suitable for clinical grade ^{90}Y generation, are discussed in this article.

Separation and purification of ^{90}Sr from HLLW

HLLW obtained from recycling of spent fuel is subjected to three-cycle solvent extraction processes at WIP, Trombay. In first cycle, depletion of residual uranium and plutonium from the waste is carried out using PUREX solvent. Uranium and plutonium from organic phase are stripped in aqueous phase using dilute HNO_3 and sent back for recycling. The U/Pu lean raffinate phase from first cycle is subjected to second solvent extraction cycle wherein indigenously synthesized 1,3-dioctyl oxy calix[4] arene-crown-6 (CC6), in isodecanol (IDA) and n-dodecane is used for selective recovery of ^{137}Cs. Recovered Cs is used for making Cs glass pencils for blood irradiators. Raffinate from the Cs recovery cycle is subjected to tetra 2-ethylhexyldiglycolamide

(TEHDGA) in IDA and n-dodecane. In this third cycle, entire actinides/lanthanides and ^{90}Sr are extracted quantitatively in organic phase leaving raffinate stream amenable to direct dilution and dispersal. Stripping of the organic phase using dilute nitric acid generates aqueous stream rich in ^{90}Sr activity. This aqueous phase generated from stripping also contains minor actinides/lanthanides and traces of Cs activity. A solvent extraction based Plant for recovery of radionuclides from HLLW has been operated in the hot cells of WIP, Trombay (**Fig. 1**). The chemical and radiochemical composition of this aqueous phase used as feed for ^{90}Sr purification is given in **Table 1**.

Table 1. Composition of Feed used for ^{90}Sr purification

Constituents	Conc.	Constituents	Conc.
$[HNO_3]$,M	4.0	Cr, mg/L	931.4
Gross α, mCi/L	10-12	Fe, mg/L	4063
Gross β, Ci/L	20.90	La, mg/L	334
^{90}Sr, Ci/L	9.50	Mg, mg/L	7.8
^{137}Cs, mCi/L	7.50	Mn, mg/L	292.7
^{106}Ru, mCi/L	2.00	Mo, mg/L	550
Al, mg/L	48.2	Na, mg/L	285.4
Ba, mg/L	25.0	Ni, mg/L	467.1
Ca, mg/L	2440	Sr, mg/L	248
Ce, mg/L	566.4	U, mg/L	35.9

Fig. 1: Solvent extraction plant for separation of radionuclides from HLLW

^{90}Sr Purification steps

In the Process Control Laboratories of NRG, Trombay, a series of steps were followed for purification of ^{90}Sr, which are described below

STEP-1: In this step, trace impurity of ^{137}Cs is removed using granulated ammonium molybdo phosphate (AMP) column. Quantitative removal of ^{137}Cs was found in this step which not only helped in the purification of ^{90}Sr but also in the reduction of man-rem exposure in the subsequent purification steps.

STEP-2: To remove α emitters *viz.* minor actinides and traces of U and Pu, TRUEX solvent was used both in liquid-liquid extraction as well as in extraction chromatography mode. Extraction chromatography was found simpler as compared to liquid-liquid extraction. This step also removed lanthanides completely from the solution.

STEP-3: Raffinate/effluent containing ^{90}Sr in ~3-4M HNO$_3$ from STEP-2 was subjected to Sr extraction step using di-(t-butyl cyclohexano)-18-Crown-6 in IDA and n-dodecane. ^{90}Sr from organic phase was stripped quantitatively using dilute nitric acid.

STEP- 4: The stripped ^{90}Sr product obtained from Step-3 was collected and passed through a glass column containing polymeric resin (XAD) to remove dissolved organic if any. The resultant solution was evaporated to get the concentrated ^{90}Sr product using a specially designed oven having a vent connected to the hood of fume-hood to avoid contamination in the fume-hood. Radiochemical composition of the ^{90}Sr product is shown below in **Table 2**.

Further purification of ^{90}Sr from the above feed solution was carried out using radiochemical precipitation method [9] after some modification. Two Fe scavenging step at pH~9.4 by alkali followed by SrCO$_3$ precipitation after adding appropriate concentration of Fe and Sr carrier were carried out which recovered more than 80% ^{90}Sr. The final SrCO$_3$, washed in water, is dissolved in a minimum volume of 2M HNO$_3$ and adjusted to a pH of 1-2. Purified ^{90}Sr(NO$_3$)$_2$ solution was allowed to reach equilibrium and used for ^{90}Y milking by employing two stage SLM generator. ^{90}Y acetate product thus generated was found to have alpha activity of 10^{-8}Ci/Ci of ^{90}Y as assayed at RSSD, BARC at low background ZnS (Ag) scintillator counting system which was ten times higher than that required for clinical grade ^{90}Y.

Further purification of this ^{90}Sr(NO$_3$)$_2$ solution was carried out by KSM 17 based SLM technique. In this technique Sr(NO$_3$)$_2$ solution purified by radiochemical precipitation method adjusted to a pH 1-2 was used as feed and 4M HNO$_3$ as receiver phase. After about 8 h, the receiver compartment was replaced at least 6 times with fresh 4M HNO$_3$ each time retaining same ^{90}Sr(NO$_3$)$_2$ in the feed compartment. This purified ^{90}Sr-nitrate solution by SLM technique was used as feed for ^{90}Y generation after the growth of ^{90}Y activity. ^{90}Y (10^{-8}Ci α/Ci) detected earlier in ^{90}Y acetate product could be reduced to less than 10^{-9}Ci α/Ci of ^{90}Y as desired for clinical applications. This ^{90}Sr-nitrate solution was preserved and used for ^{90}Y milking as and when required after allowing it to reach radioactive secular equilibrium.

Separation of carrier-free ^{90}Y using two-stage SLM generator

A two-stage SLM based generator system developed in-house [5] is used for the separation of carrier-free ^{90}Y, which is principally based on the solvent extraction properties of two ligands, namely 2-ethylhexyl 2-ethylhexyl phosphonic acid (KSM-17) and octyl phenyl-N, N-diisobutyl carbamoyl methyl phosphine oxide (CMPO) under optimum conditions. The system was operated in sequential modes with each cell having 5mL capacity. In the first stage, the equilibrium mixture of ^{90}Sr and ^{90}Y adjusted to a pH of 1-2 was used in the feed compartment and the receiver compartment contained 4 M HNO$_3$. KSM-17 based SLM was used for selective transport of ^{90}Y to the receiver phase in about 4 h. The product from this stage was taken out and placed in the feed compartment of the second stage, whereas the ^{90}Y depleted lean ^{90}Sr left out in the feed compartment of the first stage was

Table 2. Radiochemical composition of Sr product

Analyte	Analysis
[HNO$_3$], M	8.02
^{90}Sr , Ci/L	80 -100
α-activity, Ci/L	10^{-5}-10^{-6}
γ- emitters	BDL

Stage-1   Stage-2

Fig.2: SLM based two stages for generation of carrier-free ^{90}Y

Table 3: Transport of β-activity after 4h in two stages

STAGE-1		STAGE-2	
β - activity (Ci/L)		β- activity (Ci/L)	
Feed	Product	Feed	Receiver
41.48	40.86	0.52	39.64
Yield ~98.5%		Yield ~97.01%	

transferred back to the feed reservoir for next cycle. CMPO based SLM was used for transport of ^{90}Y in second stage where 1M acetic acid was used as receiver phase. Stage 1 and 2 of the generator system are shown in **Fig. 2**. Beta activity transported after 4h are given in **Table 3**.

Experimental condition

Cell volume: 5 mL for each compartment, Feed: pH 1.24, Gross β- activity: 82.96 Ci/L, Receiver phase in 1st stage: 4M HNO$_3$, Receiver phase in 2nd stage: 1M CH$_3$COOH Thus, carrier-free ^{90}Y product of ~40 Ci/L in acetic acid medium could be generated under optimized conditions and supplied to RMC, Mumbai.

Special shielding containers were fabricated for transporting batches of ~140-160 mCi ^{90}Y from BARC,

Trombay to RMC, BARC in public domain. Approved transportation procedure by regulatory authority was followed during transportation of each lot.

Quality Control of the ^{90}Y Product

Quality Control of the final product

with respect to ^{90}Sr was carried out as per "BARC Method for Quality Control of ^{90}Y" which is based on Extraction Paper Chromatography (EPC) [10]. Paper chromatography pattern of ^{90}Y is shown in Fig. 4. The contamination of ^{90}Sr in all batches of ^{90}Y-acetate product was found within
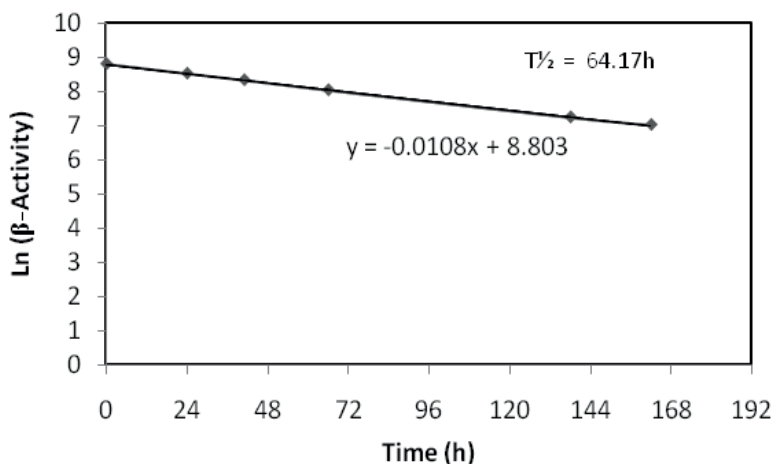

Fig. 4: Ln (β-activity) vs time plot for product in acetic acid medium

the permissible level. Fig. 4 shows the decay curve of ^{90}Y activity as a function of time. T$_{1/2}$ as calculated from the slope of the line plotted between Ln (β- activity) vs time in hour is found to be 64.17h indicating the purity of the product.

The ^{90}Y-acetate product was subjected to various quality control tests as per the requirements of Radiopharmaceuticals Committee. Typical β spectrum of ^{90}Y before and after complete decay is shown **Figs. 5 & 6.**

The elemental concentrations in six separated batches of ^{90}Y–acetate products as carried out at FRD laboratory by Inductively Coupled Plasma-Optical Emission Spectrometry (ICP-OES) are given in **Table 4.** These analysis results were validated by carrying out the analysis at WMD laboratory. Presence of elements in each batches were observed to be same as in reagent blank (1M acetic acid) indicating presence of no metallic impurities in the ^{90}Y-aceate product.

Gross α impurity analyses in six

^{90}Y-acetate batches (each about 140-160 mCi in 4 mL at the time of supply) after near complete decay as assayed by RSSD, BARC using low

background ZnS (Ag) scintillator counting system are given in **Table 5** (next page). For validating the results, one particular batch (Batch 11) of
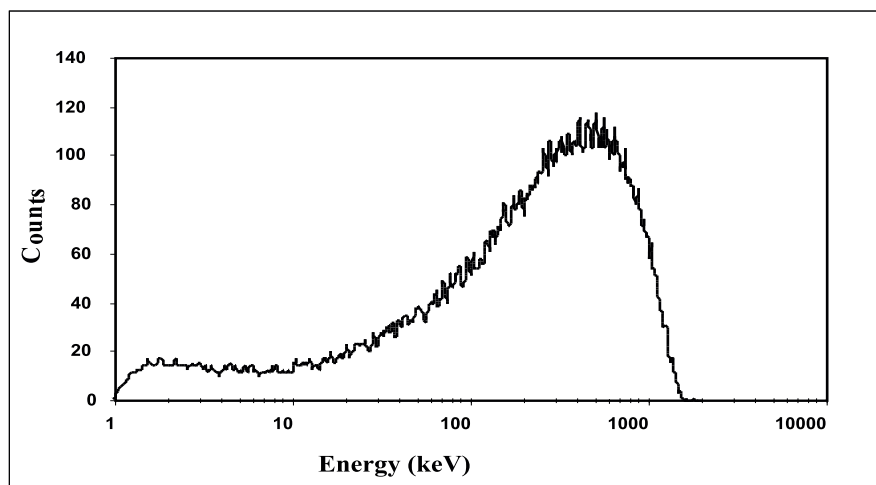
Fig. 5: β spectrum of ^{90}Y
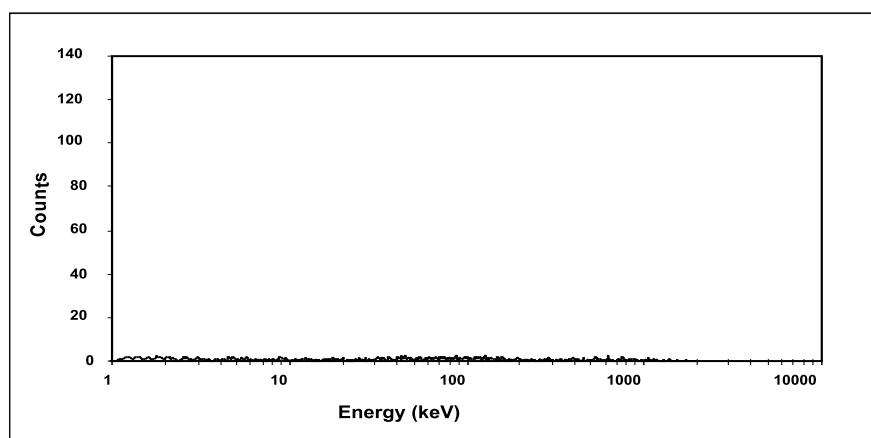
Fig. 6: β- Spectrum of decayed ^{90}Y acetate sample

Table 4: Elemental analysis of ^{90}Y- acetate samples by ICP-OES

(All values are in μg / mL on sample basis)

Element	*Blank	Batch-1	Batch-2	Batch-3	Batch-4	Batch-5	Batch-6
Al	0.052	0.069	0.074	0.055	0.056	0.049	0.056
Ca	0.900	0.807	0.878	0.890	0.940	0.910	0.940
Fe	0.020	0.024	0.027	0.020	0.022	0.021	0.022
Cu	<0.010	<0.010	<0.010	<0.010	<0.010	<0.010	<0.010
Zn	<0.020	<0.020	<0.020	<0.020	<0.020	<0.020	<0.020
Zr	<0.010	<0.010	<0.010	<0.010	<0.010	<0.010	<0.010
Pb	<0.025	<0.025	<0.025	<0.025	<0.025	<0.025	<0.025

*1M Acetic acid

Table 5: Alpha assay of decayed ^{90}Y product

Batch No.	^{90}Y ß – activity in separated product (Ci/L)	α activity in decayed ^{90}Y solution (Ci α /Ci^{90}Y)		^{90}Sr activity (Ci^{90}Sr/Ci ^{90}Y) (ß after EPC)
		RSSD*	RCD*	
9	38.90	1.65×10^{-9}	-	1.5×10^{-7}
11	38.56	0.55×10^{-9}	0.85×10^{-9}	1.4×10^{-7}
12	37.48	1.07×10^{-9}	-	1.2×10^{-7}
13	37.60	0.66×10^{-9}	-	1.4×10^{-7}
15	35.46	0.34×10^{-9}	-	1.3×10^{-7}
16	34.96	0.15×10^{-9}	-	1.4×10^{-7}

[Permissible limit-α : $<1 \times 10^{-9}$Ci α /Ci ^{90}Y, ^{90}Sr:$<10^{-6}$Ci/Ci of ^{90}Y]

*RSSD - Radiation Safety System Division
*RCD - Radiochemistry Division

Fig.7: ^{90}Sr-^{90}Y generator system housed in Fume-hood at PP

decayed ^{90}Y solution was also assayed at Radiochemistry Division, BARC, using Solid State Nuclear Track Detector (SSNTD).The result of analysis is given in the same Table. Good agreement is observed between the results obtained from both the laboratories using different counting systems.

A ^{90}Sr-^{90}Y generator system housed in Fume-hood is shown in **Fig. 7.**

Conclusions

• *HLLW is a good source for recovery of ^{90}Sr. Purification of ^{90}Sr could be done using a series of in-house developed extractants and optimized steps to achieve the level of purity required for milking of ^{90}Y.*

• *Carrier-free ^{90}Y could be successfully recovered from Sr and have a good potential use for therapeutic applications.*

• *The carrier-free ^{90}Y-acetate product having specific activity ~40Ci/L can be used for radiopharmaceutical applications. At a time, about 140-160 mCi activity could be obtained by the generator system.*

• *To meet the rising demand for ^{90}Y activity, such multiple generator systems may be employed in multiple fume hoods keeping in mind that not more than 500 mCi of ^{90}Sr activity can be handled in a particular fume-hood.*

Corresponding author and email:
Shri C.P. Kaushik (cpk@barc.gov.in)

contribution during the course of the work.

References

1. IAEA, Technical Series no. 470, Therapeutic radionuclide Generators: ^{90}Sr/^{90}Y and ^{188}W/^{188}Re Generators (**2009**).

2. P.V. Achuthan, P. S. Dhami, R. Kannan, V. Gopalakrishnan and A. Ramanujam, "Separation of

Carrier-free ^{90}Y from High Level Waste by Extraction Chromatographic Technique Using 2-ethylhexyl-2-ethylhexyl Phosphonic Acid (KSM-17)", Sep. Sci. Technol. 35(2), 261(**2000**).

3. A. Ramanujam, P. S. Dhami, R.R. Chitnis, P.V. Achuthan, R. Kannan, V. Gopalakrishnan and K. Balu, "Separation of ^{90}Sr from Purex High Level Waste and Development of ^{90}Sr-^{90}Y Generator", BARC Report, 2000/E/009.

4. A. Ramanujam, P.V, Achuthan, P.S. Dhami, R. Kannan, V. Gopalakrishnan, V.P. Kansra, R.H. Iyer, and K. Balu, "Separation of carrier-free ^{90}Y from high level waste by supported liquid membrane using KSM-17", J. Radioanal. Nucl. Chem. 247(1), 185(**2001**).

5. P.S. Dhami, P. W. Naik, N. L. Dudwadkar, R.Kannan, P.V.Achuthan, A. Dakshinamoorthy, U. Jambunathan, S. K. Munshi, P. K. Dey, Usha Pandey and Meera Venkatesh, "Studies on the Development of a Two Stage SLM System for the Separation of Carrier-free ^{90}Y using KSM-17 and CMPO as Carrier, Separation Science and Technology, 42, 5 1107-1121 (**2007**).

6. R. Chakravarty, U. Pandey, R.B. Manolkar, A. Dash, M. Venkatesh, M. R. A. Pillai, "Development of an electrochemical ^{90}Sr-^{90}Y generator for separation of ^{90}Y suitable for targeted therapy", Nucl. Med. Biol. 35(2): 245-253, Feb. **2008**.

7. P. S. Dhami, P. W. Naik, Poonam Jagasia, N.L.Dudwadkar, , R.Kannan, P.V.Achuthan, S.C.Tripathi, S. K. Munshi and P.K.Dey, Usha Pandey and Meera Venkatesh "Development of ^{90}Sr-^{90}Y Generator systems for Radio Therapeutic Applications" BARC Newsletter, Issue No.315, July-August, **2010**.

8. European Pharmacopoeia, monographs (Ed 8.2) **2014**.

9. D.N. Sunderman and C. W. Townley, The Radiochemistry of Barium, Calcium and Strontium, NAS-NS 3010, National Academy of Sciences, National Research Council, Nuclear Science Series (**1960**).

10. Usha Pandey, Prem S. Dhami, Poonam Jagasia,Meera Venkatesh, and M. R. A. Pillai, "Extraction Paper Chromatography Technique for the Radionuclidic Purity Evaluation of ^{90}Y for Clinical Use," nal. Chem. 80, 801-807(**2008**).

Challenges in Installation of Advanced Servo Manipulator in WIP Hotcell, Trombay, BARC

[1]B.N. Bhagyawant, [1]Pravind, [1]S. Patankar, [1]Suprabha, [1]R. Khokher, [1]R. Tripathi, [1]A.K. Gangyan, [1]M.K. Tiwari, [1]Jyoti Diwan, [2]S. Saini, [2]M.N. Rao, [2]R. Sahu, [1]S. Wadhwa, [2]D.D. Ray, [2]Dr. C.P. Kaushik & [3]K. Agarwal

[1]**Waste Management Division,** [2]**Division of Remote Handling and Robotics**
[3]**Nuclear Recycle Group**

Abstract

The High Level Liquid Waste (HLLW) generated during reprocessing of spent fuel is vitrified in a glass matrix at Waste Immobilisation Plant (WIP), Trombay. The handling and conditioning of HLW is carried out in Hot Cells equipped with robust remote handling gadgets like Servo Manipulators (SM)/Power Manipulators, In-Cell Cranes, Pneumatically and Electrically driven Trolleys, Impact Wrenches and various types of Grapplers, etc. An indigenously developed 1st generation SM installed in 2001 performed satisfactorily during its life span of over 15 years. The Division of Remote Handling and Robotics and the Waste Management Division jointly developed an improvised version of SM called Advanced Servo Manipulator (ASM), which was installed in the Hot Cell of WIP Vitrification Bay. The ASM is equipped with force reflection capabilities and other major improvements such as reconfigurable arm structure, higher payload and digital control to make remote operations faster, safer and accurate. Installation of the new ASM and dismantling of old SM was carried out in a limited time duration in Hot Cells in the midst of high level of background radiation. Background radiation of hot-cell was a serious concern in respect of men-rem consumption during installation work. Thus, a radiation survey was carried out followed by Decontamination (DC) exercise at certain locations where contamination was found to be very high. Later, these hot spots were covered temporarily with portable shielding. The objective of this paper is to understand challenges faced during the installation of new ASM in the Hot-cell of WIP Vitrification Bay.

Keywords: Waste Immobilisation Plant, High level liquid Waste, Vitrification, Remote handling Equipment, Servo Manipulator, Advanced Servo Manipulator, Graphical User Interface, Cable-take up System

Introduction

India has adopted "closed fuel cycle" which involves reprocessing and recycling of spent nuclear fuel. During reprocessing, Uranium & Plutonium, constituting a bulk of the spent nuclear fuel, are separated and subsequently recycled. The remaining portion constitutes high level radioactive waste (HLW) containing most of the fission products and minor actinides etc. The HLW is further vitrified either in Induction Heated Metallic Melters or in Joule Heated Ceramic Melters.

India has mastered the technology of Vitrification of HLW by employing Metallic as well as Ceramic Melters. Vitrification involves handling of high level liquid waste at high temperature (1100 ˚C), and the whole operation is carried out in a well ventilated thick concrete structure called hot-cells [1] & [3]. Remotisation is the only key for safe, efficient operation and maintenance of Vitrification facilities. It is therefore given due importance right from the stage of designing the facility to its decommissioning.

Indigenously developed 1st generation Servo manipulators have been deployed for the first time in India with reasonable degree of success in WIP, Trombay. Two servo manipulator systems are mounted on carriages to cover the entire vitrification bay. Servo Manipulator system mainly consists of Master Arms mounted on swivel plate outside the hot cells whereas servo motors, controllers & slave arms are mounted on swivel plate inside the hot cells. Master arms and slave arms are electrically coupled. Operation on master arms shall be replicated on slave arms inside hot-cells via feedback servo motors and feedback controllers. Servo Manipulator has been utilized in WIP, Trombay, for precision handling such as insertion of thermocouples, air-line connectors, guide for impact wrenches etc.
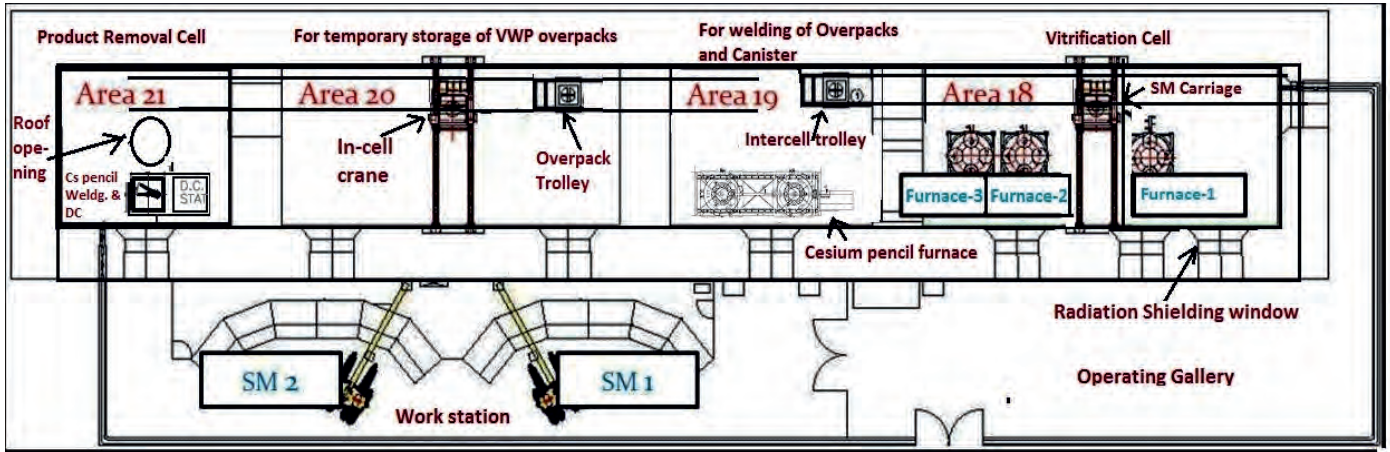
Figure 1. Layout of SM workstation and hot cell

At WIP, Trombay, the hot-cell is equipped with various remote handling equipment to carry out remote operations during production of vitrified waste product (VWP) canisters as well as for Cs glass pencil production viz. canister positioning system for pouring of HLLW in canisters, remotely operated welding machine for welding of canisters & overpacks, in-cell crane and various wall mounted manipulators for handling of Cs glass pencil and VWP canisters etc. A typical layout of hot-cells, indicating various areas along with the nature of duty is shown in the **Figure 1**. The cell has a pair of slave arms mounted on telescopic carriage for remote handling operations. This is the only facility where servo manipulator is still in use. The master arms are mounted in the operating gallery of SM workstation.

The existing pair of servo manipulator system was installed in 2001 and had performed satisfactorily during the service period. However, of late, the system fell short of desired performance levels led by frequent maintenance issues due to aging, obsolete technology, lack of spares, limited maintainability etc.

In view of aforesaid reasons, the existing Servo Manipulators had been replaced with the Advanced Servo Manipulator (ASM) system. The new ASMs are expected to result in less maintenance and score high in terms of reliability [2]. This will enhance availability of manipulator system for remote handling operations in Vitrification Cell (area 18).

Advanced Servo Manipulator (ASM)

ASM represents a new generation of servo manipulators with force feedback capabilities. The manipulator is expected to provide maintenance free operations and enhanced reliability. Force feedback makes remote operations faster, safer and precise. Other design features incorporated with ASM include higher payload capacity and Graphical User Interface (GUI) system which provide flexibility for advanced control with high degree of precision [4].

Features of ASM:

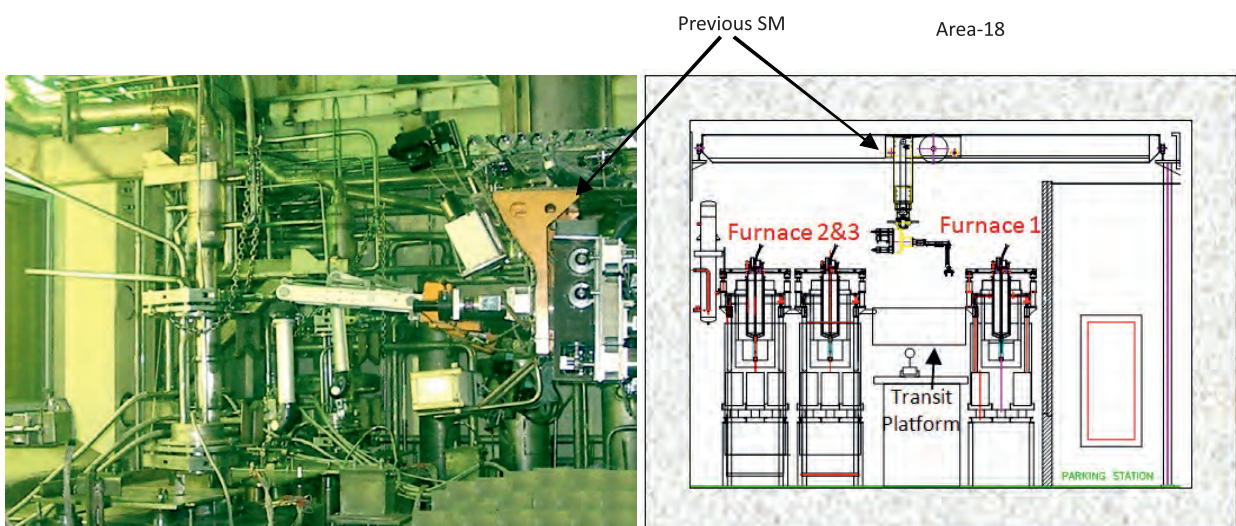• Lesser maintenance and enhanced reliability.

• Fail safe brake in motors

Figure 2. Typical layout existing servo manipulator in Vitrification cell

Figure 3 . Single pair of ASM

- Force feedback and advanced servo drive system

- Advanced and customized cable-take up system.

- Adjustable gripping force control. Force reflection capabilities available to operator.

- Resolvers are used for accurate position and velocity feedback.

- PC interface based operations along with master slave modes. Slave arm made by radiation tolerant material which is IP65 rated to enable decontamination by water spray washing.

- Easy to assemble and disassemble into sub-assemblies for maintenance.

- ASM is provided with indexing to the first three axes.

- Joints are directly coupled with motors and gear assembly, omitting requirement of wire ropes and other linkages.

Specification of ASM:

1. DOF (Degree of Freedom) » **6**

2. Payload » **25 kg**

3. Maximum reach » **1 . 0 m** from shoulder joint

4. Gripper opening » **80 mm**

5. Grip force » **320 N**

6. Force reflection ratio » **0 to 1** (with max. 8kg)

7. Slave arm cable length » **100 m**

Total seven no. of motion in ASM described as:- X-Motion (J1), Y-Motion (J2), Z-Motion (J3), Azimuth Rotation (J4), Wrist Elevation (J5) Wrist Rotation (J6), Tong Opening (J7)

GUI System:

The Advance Servo Manipulator runs on software developed in-house by DRHR. The software takes position error input from the master arm and the feedback input from slave arm. It calculates the estimated kinematics for the slave arm and sends signal to slave drives for motor control.

It can be operated in following three modes:

- User Mode

- Admin Mode

- Service Mode

Pre-installation challenges for ASM

Prior to installation of ASM, it was imperative to know the condition of Vitrification cell with respect to its background radiation & contamination level. Thus, a radiation survey was carried out and subsequently, Decontamination (DC) exercise was undertaken at certain locations where contamination level was found to be very high. Additionally, portable shielding arrangement was designed,

fabricated and installed at the site to contain the radiation streaming in working area.

a) Radiation survey

Background radiation was found very high in Vitrification cell, including few hot spots in parking area. Background radiation was a serious concern in respect of men-rem consumption during installation.

b) Decontamination

Intense decontamination (DC) was done to those radiation hot spots where the dose level was beyond acceptable limit. Specially, area around the work space of ASM installation was rigorously cleaned.

c) Portable shielding

In spite of DC, few radiation hot spots were still identified with high levels of radiation. As a result, the time available was insufficient for the workers to carry out dismantling and installation at these sites. This problem was overcome by using remotely handled portable shielding as shown in **figure 7**. It reduced men-rem consumption, thus resulting in long hours of operation. This enabled the workers to successfully carry out the required dismantling of existing Servo Manipulator and subsequent
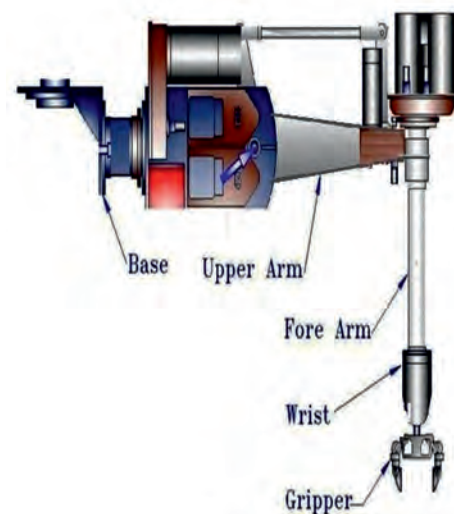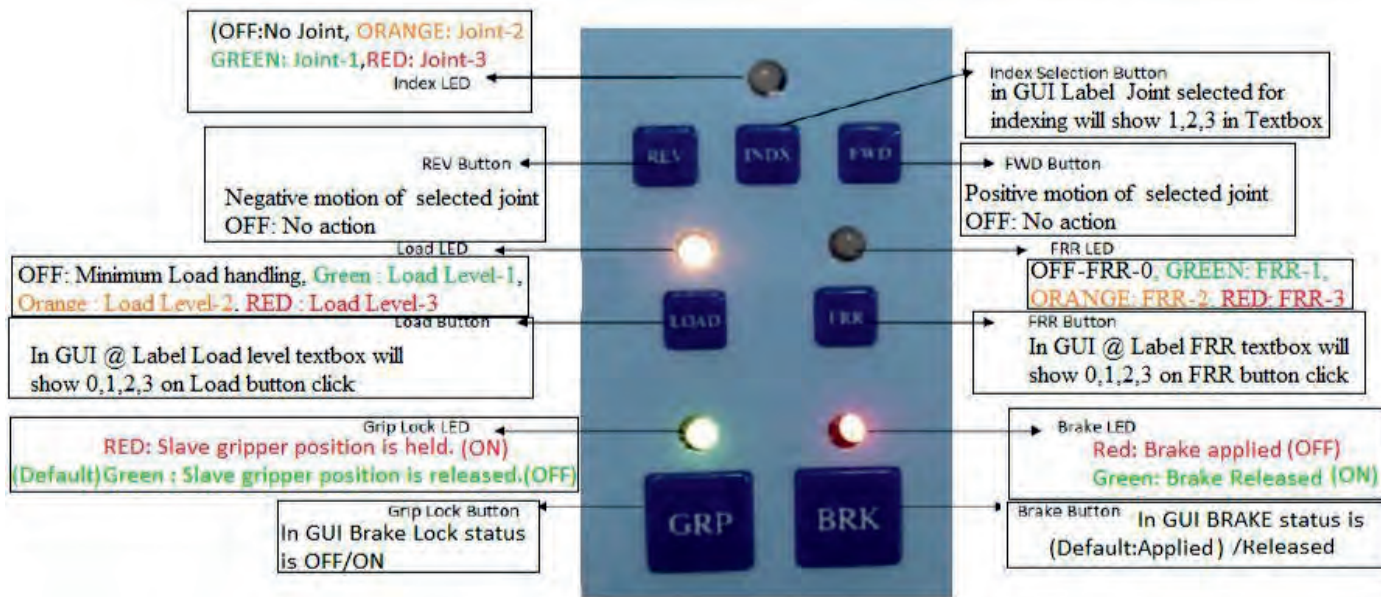

Figure 4. Slave arm schematic

Figure 5. Keypad detail of Master arm

installation of Advanced Servo Manipulator in HL bay.

Dismantling Work

1) Master arms (in Inactive area)

2) Slave arms (in Active area)

3) Accessories as control panel (Inactive Area) and cables (Master arm to Hot cell)

4) Inlet- inactive work, cell inlet to slave arm- Active work)

Generation of secondary waste

After total dismantling, the slave arm and active cables were wrapped in PVC and packed into the drums. Total twenty numbers of drums (volume 4m^3) generated of Category-1

Installation of ASM

Subsequent to dismantling, the parking area, telescopic boom along with swivel plate etc. was decontaminated prior to start of installation of ASM. Installation of ASM has been categorized into following parts:-

1) Installation of master arms in operating area.

2) Installation of control panel in operating area

3) Outside testing of assembly for readiness.

4) Installation of customized cable take-up system

i. Verification of the dimensions compatibility of cable take-up with existing booms

ii. Outside trial of cable take-up system

iii. Installation of brackets

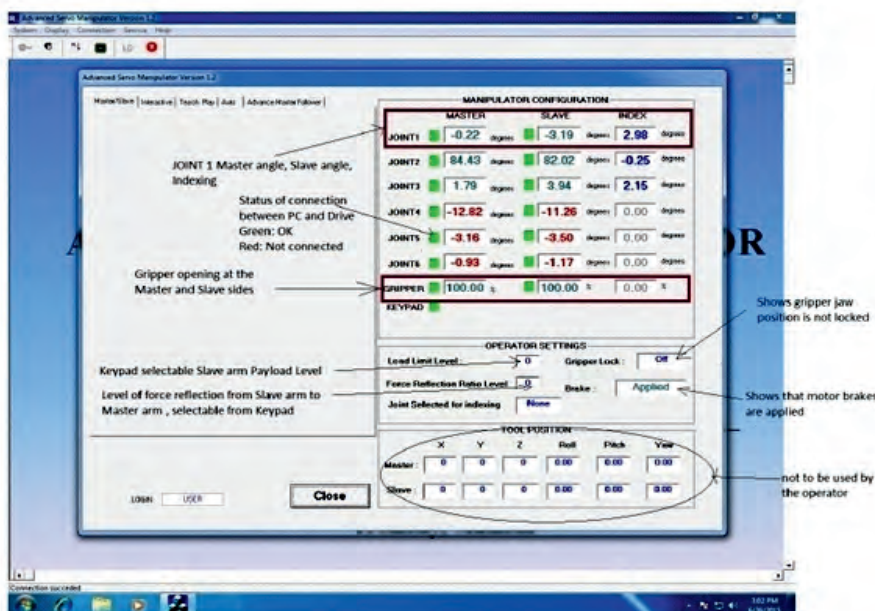iv. Testing of cable take-up system

Figure 6. Graphical User Interface

Figure 7. Portable lead shielding mounted on the cut out of wall between Melter cell and Installation site

5) Reposition the slave arms location

6) Cable routing (active + inactive work)

7) Installation of slave arms (active work)

I. Bracket installation on swivel plate

ii. Repositioning of slave arms

Transportation of Slave arm

A Slave Arm was planned for induction in the hot-cell in assembled condition. The specially designed structures on which the slave arm had to be mounted was taken to the hot cell after removing the concrete hatch block from cell top area with the help of a 40 Te crane. Subsequently, it was routed via cell maintenance area using a service crane of 1 T crane. After introduction in A-18 of hot-cell, the slave arm along with its supporting structure was shifted to installation zone utilizing a 2 T in-cell crane.

Arms installation

The arms were transferred to the parking area one-by-one with its frame structure. The frame was meant to protect the slave arms during shifting. The slave arms were installed one-by-one in assembled condition on brackets on swivel plates.

Major Challenges faced during ASM installation

a) Cabling:

A major challenge encountered during the installation was that of routing of cables through hangers 9 meters above the floor level in high radiation area. A total of thirty-two nos. of power and control cables (each with a length of 100m) were to be handled inside hot cells. These were partly addressed with the help of remote portable shielding and effective mock trials. Cable entanglement also offered a unique challenge while inserting the cables inside the cell.

b) Cable take-up system:

Retrofitting the cable take-up system was a herculean task. The hot cell environment made the dimensions measurement difficult due to protective wears and limited visibility. In spite of numerous trials at the divisional workshop to retrofit the cable take-up system within the designated space inside the hot-cell, modifications were necessitated during installation.

c) Re-orientation of slave arms:

During laying of cables for cable take-up system, the last loop of cables were found to be interfering with the motor of the swivel plate, which had constrained the movement of swivel plate & also the reach of slave arms.

To overcome this, the orientation of slave arms was changed by 180^{0} with respect to its previous orientation. To accomplish the re-orientation task, separate brackets were installed to align the holes for fastening.

Commissioning Activities:

a) Commissioning of Control Panels

In ASM, the Master and Slave arm were connected through electrical cables, and the slave arm is powered by servo motor. The electrical and control systems of the ASM consists of motors, feedback devices, sensors, controller, keypad, human-machine-interface (HMI). After connecting all cables of slave arm and master arm with control panel, a trial was carried out to check the electrical

Master arm dismantling from swivel plate

Disconnection of motor cables

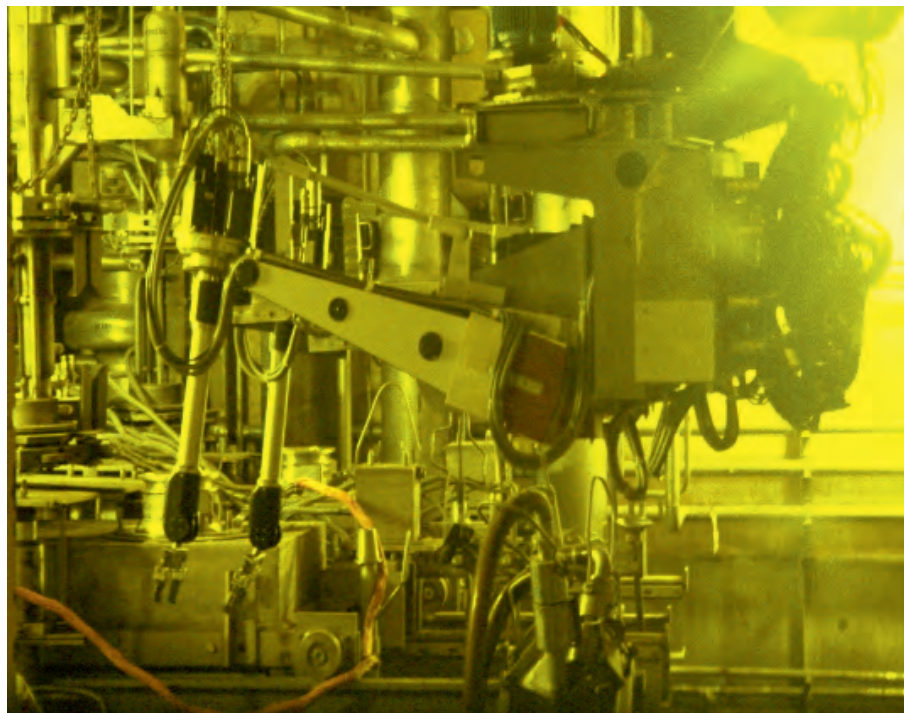**Figure 8. Dismantling work of master arms**

Figure 9. Installed slave arms of ASM in hot cell

At times, the entire range of gripper jaws could not be achieved. Proper earthing was carried out to rectify the issue and avoid noise.

Critical operations accomplished by ASM after installation

a) Refurbishment of Induction furnaces

The pneumatic cylinder of the lifting device was jammed of furnace II & furnace III. A specially designed tools was developed and with the help of ASM, the tool was guided precisely at specific location which was inaccessible by any other method and both furnace's could be retrieved for further production of vitrified waste canisters and vitrified Cs glass pencils.

b) Insertion of thermocouple

Thermocouple of furnace II was bent enough, which was not aligned over thermo-well by in-cell crane. Thus, thermocouple was inserted in existing induction furnace assembly using in-cell crane & ASM.

connectivity. During trials, some abnormal functions were found and to rectify thisthe entire control panel was checked fully once again and it was found that the three connectors were not properly placed in their location. Interchanged with each other. Later, this was corrected and installed in a right position.

b) Commissioning of ASM

ASM was subjected to rigorous testing by repeated regular guiding operations in hot cell to verify any

kind of malfunctioning. During testing, reaches of all joints and smoothness in motion as well as force reflection features were thoroughly checked.

During testing, few problems such as;

1) Over-shooting, jerking and over exceeding the range of slave arms, which was corrected by updating the drives software.

2) Joints such as J2 (Y-motion), J3 (Z-Motion) etc used to stop functioning occasionally.

Summary

a)This entire work right from dismantling of existing SM to installation followed by testing and commissioning of ASM was carried out efficiently within 60 days.
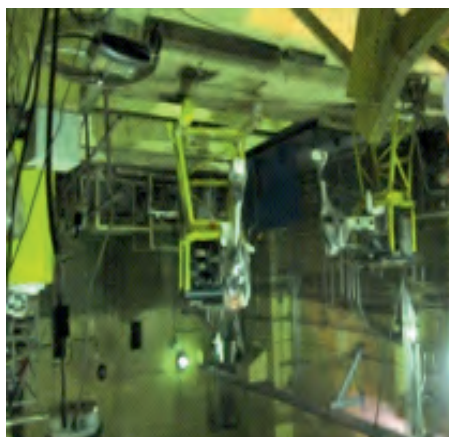

Figure 10. Inactive cabling

Figure 11. Cable take-up installation inside the hot-cell

| Cell top to Area 55 | Area 55 to Vitrification cell | Lowering arm in Vitrification cell |

Figure 12. Transportation of Slave Arms from inactive to active area

b)As against the estimated men-rem consumption of 338 person-mSv actual man-rem consumption turned out to be only 82 person-mSv.

Corresponding author and email: Shri S.Wadhwa (swadhwa@barc.gov.in)

Acknowledgements

Authors sincerely acknowledge the contribution made by entire crew members of the respective sections of WMD as well as DRHR during the installation of ASM.

References

1. C.P. Kaushik, Indian Program for Vitrification of High Level Radioactive Liquid Waste, Procedia Materials Science (**2014**)

2. K. Jayarajan, D.D. Ray and Manjit Singh, "Advanced Servo Manipulator: A milestone in Remote handling Technology", BARC Newsletter (**2007**).

3. C.P. Kaushik, Amar Kumar, Neelima S. Tomar, S. Wadhwa, Darshit Mehta, R.K. Mishhra, Jyoti Diwan, Suresh Babu, Sk. Marathe, A.P. Jakhete, Savita Jain, Anand G. and Kailash Agarwal, "Recovery of Cesium from High Level Liquid Radioactive Waste for Societal Application: An important Milestone" BARC Newsletter (**2007**).

4. K. Jayrajan, J. K. Mishra, D. D. Ray, M. N. Rao, D. Biswas and Manjit Singh, "Development of Advanced Servo Manipulator for Remote Handling in Nuclear Installations, Proceedings of the National Conference on Robotics and Intelligent Manufacturing Process", Hyderabad (**2009**).

5. Waste Immobilization Plant, Safety Report and Technical Specification (**2011**).

Figure 13. Bracket for re-orientation of Slave arm

Figure 14. Commissioning of ASM

Central Complex at BARC